NUCLEAR INSTRUMENTS AND METHODS 137 (1976) 473–516; © NORTH-HOLLAND PUBLISHING CO.

ANALYTICAL APPLICATION OF PARTICLE INDUCED X-RAY EMISSION

SVEN A. E. JOHANSSON and THOMAS B. JOHANSSON

Department of Nuclear Physics, Lund Institute of Technology and University of Lund, Sölvegatan 14, S-22362 Lund, Sweden

Received 31 May 1976

This review article deals with the X-ray emission induced by heavy, charged particles and the use of this process as an analytical method (PIXE). The physical processes involved, X-ray emission and the various background reactions are described in some detail. A theoretical discussion of the sensitivity is given. Experimental arrangements are described and various practical problems are discussed in considerable detail. Results on sensitivity, accuracy and precision so far obtained are reviewed. A large number of applications in various fields are described, especially in biology, medicine and environmental sciences. A comparison with some other analytical methods is made.

1. Introduction

For a long time X-ray emission has been used for analytical purposes, mainly in the form of X-ray fluorescence analysis. It is a well-known fact that the cross section for X-ray emission in charged particle bombardment is quite high. In 1970 it was experimentally shown by Johansson et al.[1]) that a combination of X-ray excitation by protons and detection by a silicon detector constitutes a powerful, multielemental analysis method of high sensitivity. Watson et al.[2]) and Flocchini et al.[3]) demonstrated that α-particles could also be used for this purpose. In papers published during the following two years Duggan et al.[4]). Johansson et al.[5]), Deconninck [6]), Verba et al.[7]), Gordon and Kraner[8]), Demortier et al.[9]), Kliwer et al.[10]), Pape et al.[11]). Saltmarsh et al.[12]), Umbarger et al.[13]), Young et al.[14]) and Barnes et al.[15]) verified and extended the earlier results and discussed various applications of the method. Since then, many papers have appeared in which the method is discussed on different levels of detail and in which a great number of applications are described.

The purpose of the present paper is to review particle induced X-ray emission (abbreviated PIXE) and its use for analytical purposes. A discussion of the physical background and the basic principles of the method is included. Experimental arrangements and technical details are discussed in considerable detail, which might be of special interest for those who are already working in the field or planning to do so. A large number of practical applications are briefly described with the aim of illustrating the usefulness of PIXE.

2. Basic principles of the method

The main features of PIXE can best be described by comments to a schematic diagram (fig. 1). A beam of protons, α-particles or heavy ions passes through an irradiation chamber. The intensity of the beam is made uniform by means of a diffuser foil or two pairs of electrostatic deflector plates sweeping the beam in two perpendicular directions. The beam is then defined by a series of collimators. The target is typically a thin foil of carbon or plastic upon which the sample to be analysed has been deposited. Thick targets such as sections of organic tissue or powder compressed to a pellet may also be used. The beam is dumped in a Faraday cup connected to a beam integrator. X-rays emitted by the sample pass through a thin window in the chamber and are detected by a silicon detector. The pulses from the detector are analysed in a multichannel analyser.

A typical spectrum is shown in fig. 2. It consists of a number of peaks corresponding to the K_α and K_β X-rays of the elements indicated in the figure. For the heaviest elements the cross-section for K X-ray production is very small but instead the L X-rays turn up in the spectrum as shown for lead. The peaks are superimposed upon a continuous background originating mainly in the backing material.

The number of counts in a peak is a measure of the amount of the corresponding element in the sample. Since all the parameters determining the X-ray yield

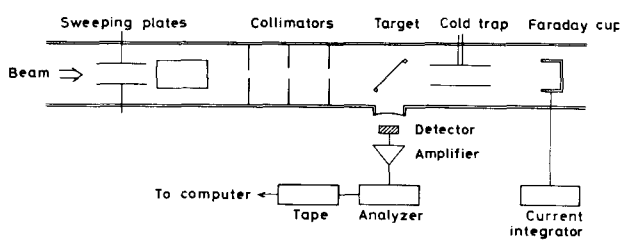

Fig. 1. A schematic diagram of the experimental arrangement.

are either known or can be measured, an absolute determination of the quantities of different elements in the sample is possible. Using a computer and a program designed to analyse this type of spectra, a printout with the composition of the sample can be obtained a few minutes after the end of a run.

At the low energy end of the spectrum there is a cut-off. This is due to the absorption of the X-rays in the windows of the chamber and the detector. With a standard arrangement, this effect sets a lower limit to the detectable elements at around aluminium. With a special detector, the useful range can be extended down to the lightest elements. This possibility of covering practically the entire periodic system in one single determination is a major advantage of PIXE. A description of the PIXE method can also be found in review papers by Folkmann[16]), Lukas[17]) and Valković[18]).

The energy of the incident particles is usually in the range 1–5 MeV/amu. However, parallel to the development of PIXE for general trace element analysis there has been a considerable amount of work on X-ray emission by low energy particles, in the 100 keV range. Such particles have a very small penetration in matter and they are therefore mainly of interest for surface studies. The emphasis has often been on light elements and, as detectors, proportional counters and crystal spectrometers as well as solid state detectors have been used. This interesting development, which has many applications in solid state physics, will not be included in the present article.

3. Production of X-radiation

The interaction between accelerated, heavy charged particles and target atoms may lead to the emission of characteristic X-rays. This phenomenon, involving the removal of at least one inner-shell electron, has been studied since its discovery by Chadwick in 1921. In theoretical descriptions the process is visualized as Coulombic and its major features are well understood. It is useful to make a distinction between point charge particles such as protons and alphas on one hand and heavier ions on the other, since the principles of interaction between incident particles and target atoms are different in these cases. A review of the inner-shell vacancy production in ion-atom collisions is given by Garcia et al.[19]). For analytical purposes, only protons and alphas are of immediate interest. Heavier ions, however, show many interesting properties and may be used for special analytical tasks, although they involve less well-known problems such as X-ray energy shift and changing fluorescence yields due to multiple ionization. For surface studies they are attractive in some cases where the particle penetration depth is critical. For low energy applications, selective ionization occurs but this has not yet been utilized analytically.

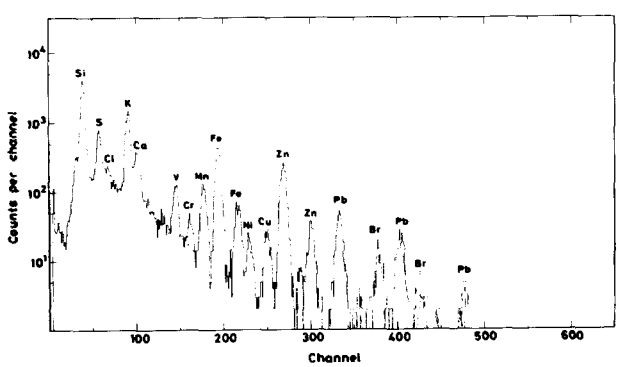

Fig. 2. A PIXE spectrum of a sample of aerosol particles with sizes between 0.25 and 0.5 μm. The proton energy was 2 MeV and the accumulated charge 40 μC.

3.1. Protons and α-particles

Merzbacher and Lewis[20]) presented a comprehensive quantum-mechanical treatment of inner-shell ionization by protons and alphas in terms of the plane wave Born approximation (PWBA) in their review of the field in 1958. This approach explains the dependence of ionization cross sections on particle energy quantitatively at higher particle energies, while in the lower energy region corrections for the binding energy of the target atom electrons and the Coulombic deflection of the particle must be considered in order to obtain a quantitative description of the process[21]).

In 1959 Bang and Hansteen[22]) published a semiclassical treatment using impact parameter and taking the particle deflection into account. Their approach describes the total cross sections quite well[23]) but has not yet been experimentally tested in detail.

Another classical approach to describe the ionization process was used by Garcia[24]) in 1970. He based his model on the binary encounter approximation (BEA) between a free electron and the incident particle. This model also considers the particle deflection and gives good agreement with experimental results. Hansen[25]) recently introduced a constrained BEA and obtained improved agreement for low particle energies. Hansteen[26]) has reviewed current ideas on ion-atom collisions.

Experimental results up to 1973 have been collected by Rutledge and Watson[27]). Most of these data refer to protons of energies less than a few MeV. Later

TABLE 1

Recent X-ray production studies. All work referred to utilized thin targets and Si(Li) detectors.

Author and ref.	Particle	Energy (MeV)	Line
Bissinger et al.[176])	p	0.5 - 3	L
Liebert et al.[35])	p	2.5 -12	K
Lear and Gray[36])	p	0.5 - 2	K
Busch et al.[31])	p	0.5 -14	L, M
Bearse et al.[33])	p	1.0 - 3.7	K, L
Gray et al.[177])	p	0.5 - 2	K
Shafroth et al.[31])	p	0.5 -30	L
Akselsson and Johansson[37])	p	1.5 -11	K, L
Criswell and Gray[36])	p	0.4 - 2	K
Ishii et al.[178])	p	1.4 - 4.4	K, L
Tawara et al.[179])	p, ^{3}He	1.4 - 4.4	K, L
Khelil and Gray[180])	p	0.6 - 2	K
McDaniel et al.[181])	α	0.5 - 2.5	K
Tawara et al.[182])	p	1.0 - 4.5	L
	^{3}He	3 - 9	
Chaturverdi et al.[183])	p	3 -12	L
	^{16}O	15 -40	
Ishii et al.[184])	p	1.0 - 4.5	M
	^{3}He	3 - 9	
Tawara et al.[185])	p	0.75- 4	K
	^{3}He	3 -12	
Milazzo and Riccobono[186])	p	0.95	K, L
Chen et al.[187])	p	0.4 - 2.0	L
Soares et al.[188])	α	1.0 - 4.4	K

experimental work in the MeV range is summarized in table 1. Comparisons between the available theories [24,28]) and experiments are typically good to 10–30% in the energy and Z regions of interest. This is not sufficient for accurate chemical analysis by PIXE. We have therefore developed a semiempirical formula for ionization cross sections based on recent thin target measurements. As pointed out by Garcia, the binary-encounter model offers a scaling law for the cross sections including only electron binding energy and particle energy. A universal curve is thus obtained if $u_i^2\sigma$ (i = K or L) is plotted vs $E/\lambda u_i$ where u_i is the electron binding energy, E the proton energy and σ the ionization cross section and λ the ratio of the proton mass to the electron mass.

In fig. 3 we plot data from thin target measurements of K and L X-ray ionization measurements from refs. 4, 29–37. The curves are fitted using a fifth degree polynomial. The curves are

$$^{e}\log(\sigma u_i^2) = \sum_{n=0}^{5} b_n x^n, \qquad (1)$$

where the coefficients b can be found in table 2 and $x = {}^{e}\log(10^{-3}E/\lambda u_i)$. u_i is the ionization energy in eV and E the proton energy in eV. The unit of the ionization cross section is 10^{-14} cm^2. u_L was calculated from

$$u_L = \tfrac{1}{4}(u_{L1} + u_{L2} + 2u_{L3}). \qquad (2)$$

A one-sigma confidence interval for the theoretical regression curve was calculated. For $E/\lambda u_i$ values between 0.034 and 0.92 and for i = K it is better than 1% and at the end-points better than 5%. For i = L, the curve is better than 2% for $E/\lambda u_L$ between 0.084 and 2.33 and better than 8% at the end-points of the curve. Tables 3 and 4 present selected cross sections for some elements.

The function used for the fitting is the same as used by Akselsson and Johansson[37]) for their K-ionization

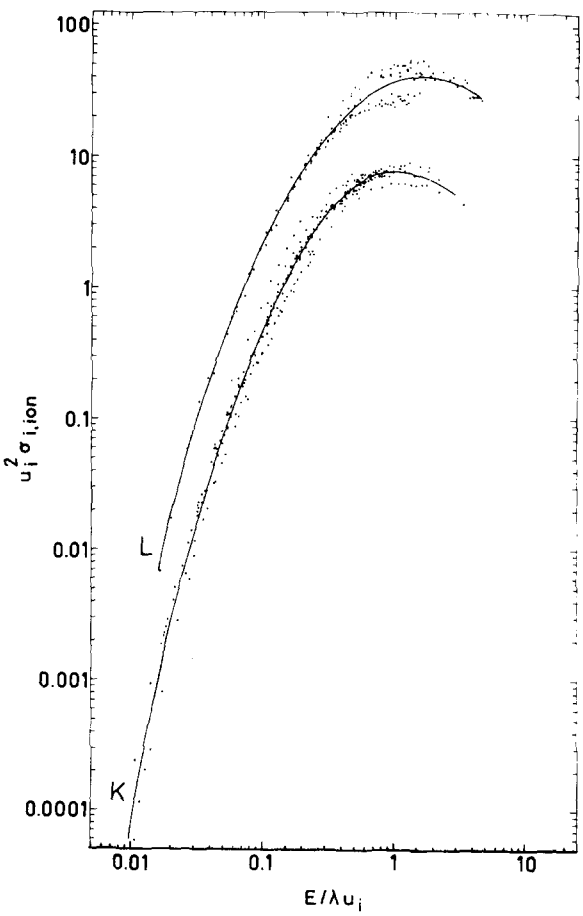

Fig. 3. A plot of the K and L ionization cross sections in proton impact. On the y-axis is plotted $u^2\sigma$, where u is the electron binding energy and σ the cross section. On the x-axis is plotted $E/\lambda u$, where E is the proton energy and λ the ratio of the proton mass to the electron mass. The dots are experimental values from recent thin target measurements. The curves are fifth degree polynomials defined in the text and in table 2.

TABLE 2

Coefficients for the calculation of X-ray production cross sections using expression (1).

X-ray	No. of points	Coefficient b_0	b_1	b_2	b_3	b_4	b_5
K	316	2.0471	−0.65906 (−2)	−0.47448	0.99190 (−1)	0.46063 (−1)	0.60853 (−2)
L	158	3.6082	0.37123	−0.36971	−0.78593 (−4)	0.25063 (−2)	0.12613 (−2)

formula. The use of many more data points in this work changes the coefficients slightly but the curve is still within the experimental errors of Akselsson and Johansson.

PWBA theory predicts a Z^2 dependence of the cross section[20]), but although the gross behaviour of experimental proton and alpha cross section data is very similar, a detailed comparison shows that deviations occur. Garcia et al.[19]) have reviewed the differences.

Eq. (1) has been obtained using proton data only. However, it can be used also for estimating ionization cross sections for alpha particle impact by scaling to equal velocity ions, but the degree of accuracy is then reduced to the order of some tens of percent.

For use in chemical analysis, the production rather than the ionization cross sections is of interest. The X-ray production cross section, σ_p, for a line in a spectrum is obtained as

$$\sigma_p = \sigma_{ion}\omega k, \tag{3}$$

where ω is the fluorescence yield and k the relative line intensity of possible transitions to fill an inner-shell vacancy. Bambynek et al.[38]) have reviewed X-ray fluorescence yields and Coster–Kronig transitions and present useful tables. Freund[39]) recently collected experimental values for K-shell fluorescence yields.

An important characteristic of X-ray spectra is the occurrence of several peaks from every element present in a sample. As discussed below, unravelling of complex spectra makes use of the relative line intensity for each element. When point-charged particles are used for excitation, the emission rates are the same as those for X-ray and electron excited characteristic X-rays from the same element. Scofield[40]) has treated the emission rates for K X-ray emission theoretically and drawn comparisons with available experimental results. His work gives agreement between theory and experiment within experimental errors for Z values between 10 and 98. For L and M X-ray emission rates the available data are scarce. More information is also needed on relative L/K, M/K and L/M emission rates. L X-ray transition probabilities are published by Salem et al.[41]). The references in table 1 to work on L and M X-ray cross sections generally also contain information on relative line intensities.

3.2. HEAVY IONS

In the previous section it was stated that for equal velocity ions the cross section for X-ray production is proportional to Z^2. This scaling law can be used to obtain rough estimates for heavy ions but a number of additional effects should be considered.

When a heavy ion passes a target atom the high Z leads to a polarization of the atomic shell. This gives an increased cross section for vacancy production. Two other effects work in the opposite direction. In order for the incident ion to be effective in knocking out an electron from the inner shells, it must come close to the nucleus of the target atom. This gives an increased effective binding energy of the electrons and consequently a lower cross section. Furthermore, it is necessary to correct for the deflection of the incident ion in the Coulomb field of the target nucleus. This leads to smaller probabilities for close encounters and hence smaller cross sections.

When an incident heavy ion collides with a target atom there is an interaction between the two electron systems. This can give rise to a transfer of a K electron from the target atom to a hole in the shells of the incident ion. This, of course, gives a contribution to the ionization cross section. An even more complicated effect was first observed in a study of the X-rays emitted in the slowing down of fission fragments. It turns out that the X-ray yield exhibits peaks for certain stopping materials. An analysis shows that the ionization cross section has a maximum when the binding energy of the electron being excited is equal to some electron binding energy in the collision partner.

A more general interpretation of these data can be made in terms of the molecular orbit theory. It is assumed that at lower velocities the electron systems of the two colliding atoms adiabatically transform to a transient molecular system. In a level diagram exhibit-

TABLE 3

K_α X-ray production cross sections in barns as calculated by expressions (1) and (3).

Element	Z	ω_K[a]	K_β/K_α[b]	Proton energy (MeV) 0.5	1.0	1.5	2.0	2.5	3.0	3.5	4.0	4.5	5.0	6.0	7.0	8.0	9.0	10.0
Al	13	0.0357	0.0134	219	625	906	1054	1113	1120	1100	1066	1027	985	910	847	797	–	–
S	16	0.0761	0.0659	68.2	257	473	638	736	832	877	899	905	900	873	834	792	753	717
Ca	20	0.163	0.1315	15.2	80.3	174	274	366	446	511	564	604	634	671	684	682	672	657
Ti	22	0.219	0.1355	7.51	45.2	106	176	248	315	374	425	469	504	556	586	601	606	603
Cr	24	0.282	0.1337	3.79	25.7	64.5	113	166	218	268	313	354	389	446	486	512	527	535
Fe	26	0.347	0.1391	1.90	14.5	38.6	70.9	108	146	185	222	256	287	341	383	414	436	451
Ni	28	0.414	0.1401	0.961	8.25	23.3	44.5	69.9	97.6	126	155	182	209	256	295	327	352	371
Zn	30	0.479	0.1410	0.485	4.69	14.0	27.7	44.8	64.2	85.0	106	128	148	187	222	251	275	295
As	33	0.567	0.1560	0.168	1.96	6.32	13.2	22.3	33.0	45.0	57.8	71.1	84.5	111	136	159	179	197
Br	35	0.622	0.1683	0.0829	1.10	3.75	8.11	14.0	21.2	29.4	38.4	47.9	57.7	77.6	97.1	116	133	148
Sr	38	0.691	0.1831	0.0284	0.466	1.72	3.90	6.98	10.9	15.4	20.6	26.2	32.1	44.6	57.4	70.0	82.2	93.6
Mo	42	0.764	0.1981	0.00678	0.151	0.621	1.50	2.81	4.53	6.63	9.07	11.8	14.8	21.3	28.3	35.6	42.9	50.0
Ag	47	0.830	0.2130	0.00111	0.0376	0.180	0.472	0.932	1.57	2.37	3.34	4.45	5.71	8.56	11.8	15.3	18.9	22.7
Sn	50	0.859	0.2230	–[c]	0.0163	0.0862	0.238	0.487	0.839	1.29	1.85	2.51	3.25	4.98	6.99	9.21	11.6	14.1
Ba	56	0.901	0.2433	–	0.00310	0.0203	0.0626	0.137	0.249	0.399	0.589	0.818	1.09	1.73	2.51	3.41	4.41	5.49
Pb	82	0.968	0.2821	–	–	–	0.246 (−3)	0.799 (−3)	0.00189	0.00370	0.00638	0.0100	0.0148	0.0278	0.0458	0.0692	0.0979	0.132

[a] "Fitted" values from Bambynek et al.[38]).
[b] Ref.: Scofield Phys. Rev. **A9** (1974) 1041.
[c] "–" denotes value outside range of formula validity.

TABLE 4

L X-ray production cross sections in barns as calculated by expression (1).

Element	Z	$\overline{\omega_L}$[a]	Proton energy (MeV) 0.5	1.0	1.5	2.0	2.5	3.0	3.5	4.0	4.5	5.0	6.0	7.0	8.0	9.0	10.0
Zn	30	0.0059	576	1253	1678	1917	2038	2086	2086	2058	2012	1956	1828	–[b]	–	–	–
Br	35	0.020	450	1212	1836	2292	2609	2823	2960	3041	3080	3089	3046	2954	2839	2713	2584
Zr	40	0.031	175	572	965	1299	1569	1782	1947	2072	2165	2233	2310	2332	2319	2283	2232
Ag	47	0.060	60.5	250	479	704	910	1092	1251	1386	1502	1599	1749	1851	1916	1954	1972
Sn	50	0.079	39.0	178	359	546	725	889	1036	1167	1282	1383	1545	1665	1752	1812	1851
Ba	56	0.120	15.0	83.3	185	300	418	534	643	746	840	927	1077	1200	1300	1379	1442
Gd	64	0.19	4.47	31.8	79.5	139	206	275	344	412	478	541	677	760	850	928	996
Hf	72	0.26	1.26	11.5	32.2	60.7	94.5	132	170	210	250	289	365	437	503	563	617
W	74	0.30	0.981	9.53	27.5	52.8	83.3	117	153	190	227	265	338	407	471	531	585
Au	79	0.34	0.421	4.80	14.9	30.0	48.8	70.4	93.9	119	144	170	222	272	320	366	408
Pb	82	0.38	–	3.3	10.7	22.2	36.8	53.8	72.7	92.7	114	135	179	222	263	303	341
U	92	0.50	–	0.876	3.32	7.53	13.4	20.5	28.9	38.1	48.0	58.5	80.7	104	127	150	173

[a] Estimated from Bambynek et al.[38]) (figs. 4–34).
[b] "–" denotes value outside range of formula validity.

ing the levels as a function of the internuclear distance several crossings appear. When a filled orbital crosses an unfilled one there is a certain probability for the electron to go over to the unfilled orbital. Such a process will also contribute to the X-ray production cross section and is most effective when the colliding atoms have the same charge.

Another characteristic feature in heavy ion bombardment is that the resulting X-ray spectra are more complicated than in proton bombardment. Each line in the simple, proton-induced spectrum is shifted and split up in a number of components. This broadening can amount to several hundreds of eV. The reason for this effect is that simultaneous vacancies are produced in the outer shells because of the heavy ionization, leading to a slight shift in the binding energy of the inner electrons.

Thus, it is evident that the production of X-rays in heavy ion bombardment is a very complicated process. In general, the cross sections are larger than expected from a simple scaling from proton bombardment but the exact values depend in a complicated way on the energy and on which particles take part in the collision. This enhancement is particularly large at low energies as illustrated in fig. 4. As will be shown later heavy ion induced X-ray emission has only a limited application in general trace element analysis and will therefore not be discussed further. The reader is referred to a review paper by Garcia et al.[19]) for a full account.

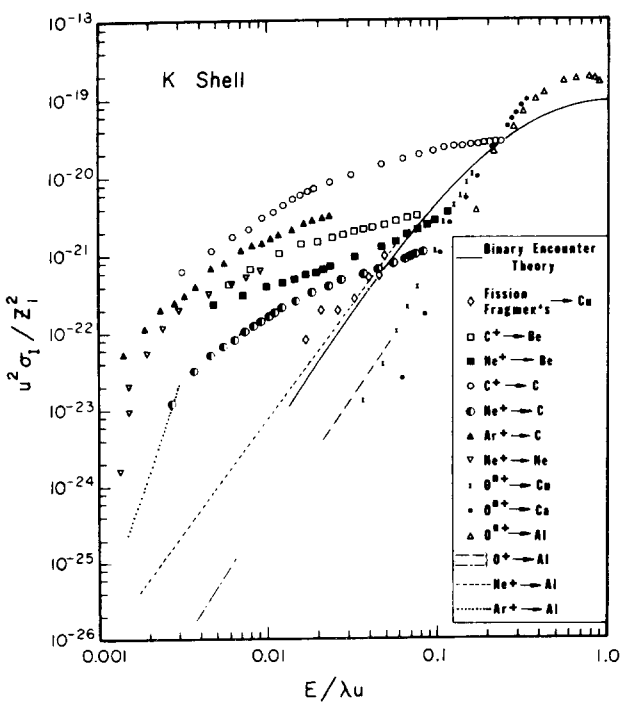

Fig. 4. Cross sections for K-shell excitation by incident heavy ions plotted in terms of the reduced parameters used in the binary encounter theory. From ref. 19.

4. Background

4.1. Protons and α-particles

In PIXE analysis the trace elements to be determined are always mixed with the bulk of the material in the sample, the so-called matrix. Examples are the organic tissue in biological samples or a carbon backing on which an aerosol sample has been deposited. The X-rays registered by the silicon detector are not only characteristic X-rays from the trace elements but also background radiation from the matrix. As an illustration of this, fig. 5 shows a spectrum of a thin carbon foil bombarded with 1.5 MeV protons. It consists of a continuous distribution peaked at rather low energy and having a high energy tail. The shape at low energies is influenced by the cut-off due to absorption in the windows of the experimental set-up.

Several processes can contribute to the background. One is bremsstrahlung from the incident particles. The cross section for this process is given by the formula

$$\frac{\mathrm{d}\sigma}{\mathrm{d}E_X} = C\,\frac{AZ^2Z_1^2}{EE_X}\left(\frac{Z}{A}-\frac{Z_1}{A_1}\right), \tag{4}$$

where Z, A and E are the charge, mass and energy, respectively, of the incident particle and Z_1 and A_1 the charge and mass of the matrix atoms. C is a slowly varying factor.

The contribution to the background arising from this process is indicated by a line in fig. 5. Apparently, the high energy part of the background can largely be attributed to this process. An important point is that the yield increases with decreasing particle energy according to the above formula. This behaviour is contrary to these of the characteristic X-ray yield and of the other background processes discussed below. Another interesting point is the term $(Z/A-Z_1/A_1)$. If the ratio Z/A is the same for the projectile as for the matrix atoms, the yield of the projectile bremsstrahlung vanishes. For most matrices the charge to mass ratio is close to 1/2. This means that this background contribution vanishes for α-particles and heavier ions but not for protons. This effect has been experimentally verified by Watson[42]) (fig. 6).

The low energy background can be attributed to secondary electron bremsstrahlung. One reason for

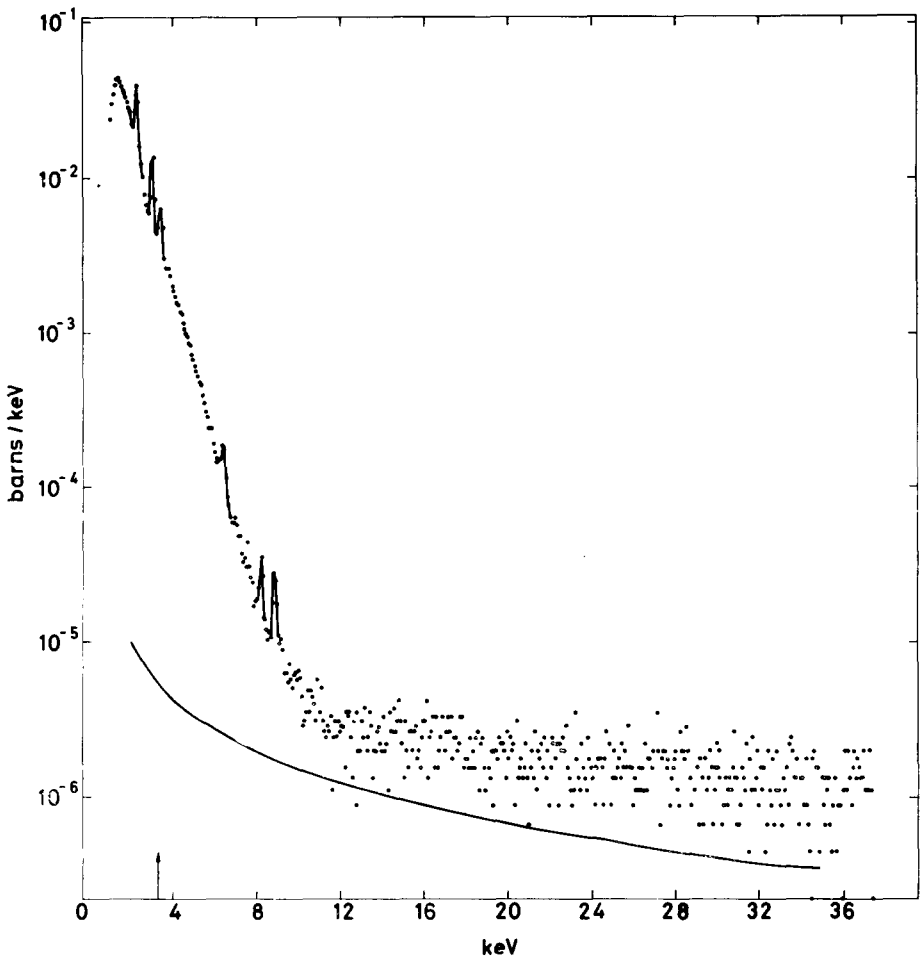

Fig. 5. Spectrum of a thin carbon foil bombarded with 1.5 MeV protons. The line shows the contribution from the proton induced bremsstrahlung according to eq. (4). The arrow indicates the maximum energy of the bremsstrahlung produced by secondary electrons.

this assumption is the fact that the bremsstrahlung spectrum decreases rapidly above an X-ray energy of

$$E_X \approx \frac{4m}{M} E,$$

which is the maximum energy transfer from a projectile of mass M and energy E to a free electron of mass m. In fig. 5 this limiting energy is indicated by an arrow and the sharp decrease above this energy is obvious. Detailed calculations by Folkmann et al.[43]) confirm that the low energy part of the background can indeed be attributed to bremsstrahlung from secondary electrons.

It is interesting to note that bremsstrahlung production by secondary electrons in the matrix is closely related to the production of characteristic X-rays of the trace elements. In both cases the primary process is the generation of vacancies in the electron shells by the incident particles. This means that the ratio of the X-ray peaks to the bremsstrahlung background is the same for all particles with the same velocity. Hence as long as the electron bremsstrahlung is the dominant part of the background, all heavy particles give the same signal to noise ratios. This will be discussed later in more detail in connection with an account of the sensitivity of the method.

The fact that electron bremsstrahlung production is a two-step process makes it possible in principle to decrease its relative yield by using extremely thin targets. The secondary electrons will then have a large probability for leaving the target without producing any bremsstrahlung. However, as found by Folkmann and also in our laboratory, the thicknesses needed for a noticeable effect are so small that such targets would be extremely difficult both to prepare and to handle.

When the incident particles have a sufficiently high

energy to excite the nuclei in the target, γ-radiation will be emitted, giving rise to a high energy tail in the spectrum due to Compton scattering in the detector. The amount of γ-radiation produced depends on the exact composition of the target. Some nuclides have a high cross section for γ-emission. One example is fluorine excited by proton bombardment for which even 1 MeV protons give a substantial yield. Furthermore, even if the detector is shielded from direct γ-radiation from the target chamber, γ-radiation can reach the detector after multiple scattering. This means that the γ-ray background will depend on the details of the experimental set-up. An obvious requirement is that γ-radiation from collimators and the beam-dump shall not be able to reach the detector. For these reasons, it is not very surprising to find that the amount of γ-ray background differs considerably in different experimental arrangements.

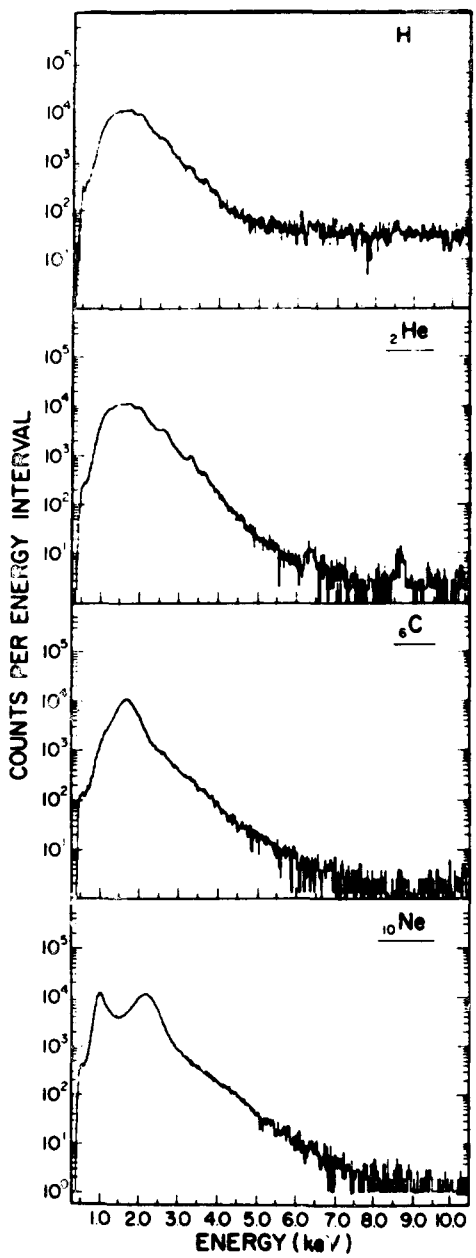

Fig. 6. X-ray spectra produced during the passage of 1.7 MeV/amu particles through a 530 μg/cm^2 mylar foil. From ref. 42.

The importance of the γ-ray background can be seen in the work of Folkmann et al.[44]). It is dominant for $Z > 30$ at proton energies of 3 and 5 MeV. Therefore, the bombarding energy must be as low as possible for minimum γ-ray background, while still giving a reasonably large characteristic X-ray yield. One must be especially careful not to use bombarding energies above the threshold for inelastic scattering in the most abundant nuclides of the matrix, e.g. ^{12}C and ^{16}O. Protons are obviously prefereable as incident particles from the point of view of γ-ray background. For the same velocity, heavier ions like ^{4}He or ^{16}O have a higher energy and consequently a large cross section for γ-emission. This is the main reason why protons of 1–2 MeV energy are the best choice for PIXE.

4.2. Heavy ions

Heavy ions such as protons give rise to background radiation by secondary electron bremsstrahlung emission. The direct production of bremsstrahlung is small, especially for not too heavy ions, because of the term $(Z/A - Z_1/A_1)$ in the expression for the cross section [eq. (4)]. For heavier ions the neutron excess causes this term to be different from zero and in some cases directly produced bremsstrahlung has been identified.

Another important source of background radiation is the radiation emitted in filling a vacancy in the 1s molecular orbital, which exists during the collision. The energy of this orbital depends on the internuclear distance and the radiation emitted will therefore be continuous. The end-point is given by the binding energy of the 1s orbital at the closest approach of the ions and hence depends on the bombarding energy.

Heavy ion can, of course, also produce γ-radiation which gives a continuous Compton distribution in the detector. As mentioned in the previous section, the heavy ions have a higher energy and consequently a higher cross section for γ-emission compared to protons of the same velocity. This is a great disadvantage which might off-set the gain due to the Z^2 term in the cross section for characteristic X-ray production.

5. Sensitivity

One of the main advantages of the PIXE method is its high sensitivity. It is therefore of considerable importance to discuss in more detail what sensitivity one can obtain and how it depends on the various experimental parameters.

In this connection it should be kept in mind that what we are discussing here is the sensitivity in the analysis of the sample being bombarded. In the preparation of this sample it is sometimes possible to enhance the sensitivity, for example by preconcentrating a water solution or by ashing an organic sample. Hence the sensitivity referring to the original material might be higher than the figures quoted here.

There are several ways of defining the sensitivity of an analytical method. In the present context, the problem is to find small amounts of various trace elements in a certain matrix. The most basic definition of the sensitivity is therefore the minimum detectable concentration. Once it is known one can calculate the minimum detectable absolute amounts of various elements knowing the weight of that part of the sample which is irradiated by the particle beam.

If one calculates the number of X-ray pulses registered by a silicon detector in a normal geometry when a small amount of a trace element is bombarded with protons in the MeV range one finds that a sufficient number for a convenient registration is obtained even with extremely small amounts of matter, of the order of 10^{-16} g. The trace elements to be measured are, however, always contained in some matrix. It can be organic tissue or a thin foil of carbon or plastic used for collecting aerosols. As described in section 4, a background arises inevitably in the interaction of the incident particles with the matrix atoms. This background sets a limit to the sensitivity which can be obtained since, in order for a characteristic X-ray peak to be discerned, it must rise above the background in a statistically significant way.

The number of pulses in the peak, N_p, must then satisfy the relation

$$N_p \geq 3\sqrt{N_B}, \tag{5}$$

where N_B is the number of pulses in the background under the peak in an interval having a width equal to the fwhm of the peak. Since the background depends on the composition of the matrix it is impossible to give a general, simple expression for the sensitivity. However, in most cases of practical interest, the matrix is composed of carbon or organic material. Since the latter for our purpose can be approximated by carbon, it suffices to determine the background for this material. Fig. 5 shows the background for 1.5 MeV protons. In the literature one can find several other examples for different particles and bombarding energies. Knowing the X-ray production cross section (section 3.1) one can calculate the amount of a certain trace element needed to satisfy relation (5). The result of such a calculation depends on the experimental conditions. The following parameters have an influence on the sensitivity: the solid angle of the detector Ω, detector resolution ΔE, collected charge j and target thickness t. It is easy to show that the sensitivity scales as

$$\Delta E^{\frac{1}{2}}(\Omega j t)^{-\frac{1}{2}}. \tag{6}$$

In order to show what kind of sensitivity one can obtain we have somewhat arbitrarily chosen the following values: $\Delta E = 165$ eV, $\Omega = 0.003 \times 4\pi$, $j = 10\mu$C and $t = 0.1$ mg/cm^2. It should be emphasized that these figures are very conservative and reflect the conditions in routine analysis. If a very high sensitivity is needed there is considerable room for improvements.

The minimum detectable concentration obtained with the above-mentioned parameter values is shown in fig. 7 as a function of the atomic number.

Some important features in this figure are immediately obvious. All the curves, corresponding to different proton energies, have a minimum (maximum sensitivity). For lighter elements the sensitivity decreases mainly due to the fall-off of the fluorescence yield. The decreasing sensitivity for the heavier elements depends on the fact that for them the X-ray cross sections are

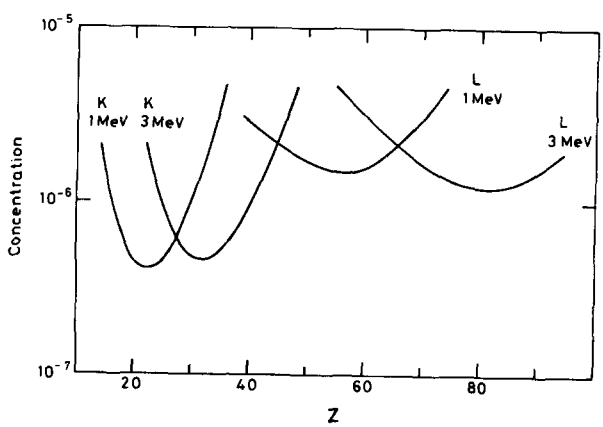

Fig. 7. Minimum detectable concentration as a function of atomic number for proton energies 1 and 3 MeV .The following experimental parameters were used: detector resolution 165 eV, solid angle $0.003 \times 4\pi$, collected charge 10 μC and target thickness 0.1 mg/cm^2.

decreasing while the background is relatively constant. Furthermore, it should be noted that the position of maximum sensitivity depends on the energy of the incident protons. Within certain limits one can therefore adjust the proton energy to give maximum sensitivity for a particular trace element. Another interesting fact of practical importance is that the highest sensitivity is obtained for $Z \approx 20$–30 which happens to be the region of greatest interest in many applications. The most suitable proton energy is then 1–2 MeV.

For heavier elements ($Z > 40$), the K X-rays give too small an intensity. Fortunately, one can in this region make use of the L X-rays, as is evident from the figure. Hence using both K and L X-rays in the analysis of a sample one can achieve a minimum detectable concentration which is fairly constant ($\sim 10^{-6}$) over practically the whole periodic table. This is a very important fact which distinguishes PIXE favourably from most other analytical methods.

There are, however, some problems in this connection. The simultaneous emission of K and L X-rays sometimes gives rise to accidental coincidences in the recorded spectra. One such example is the L_β peak of cadmium ($E = 3.317$ eV) which coincides with the K_α peak of potassium ($E = 3.314$ eV). In most cases this problem can be solved by a careful analysis of the spectra (discussed in section 7.6) but it must be borne in mind that the sensitivities shown in fig. 7 do not take into account such coincidences. Another problem is detection of very light elements. The low energy of the X-rays from these elements makes it necessary to make special arrangements on the detection side. With a standard silicon detector a reasonable sensitivity can be maintained down to sulphur or aluminium. By using a windowless detector even lighter elements can be detected. Spectra showing well defined peaks from B, C and O have been reported[45]). The detector problem is treated more fully in section 7.4.

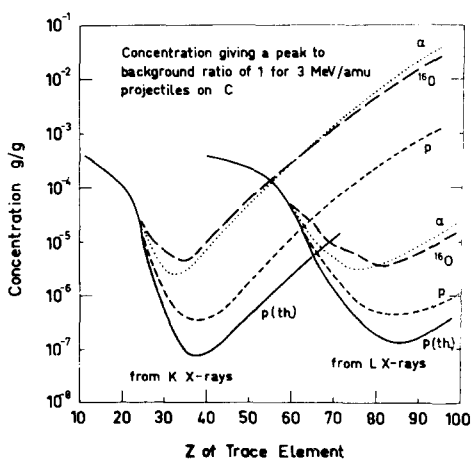

Fig. 8. Minimum detectable concentration as a function of atomic number for protons, α-particles and heavy ions with an energy of 3 MeV/amu. From ref. 44.

So far only proton excitation has been discussed. It is of interest to investigate whether excitation by α-particles or heavier ions can yield higher sensitivities. In the same way as for protons, one can do this by measuring the background of the matrix and then use the known X-ray production cross section of the trace elements to compute the sensitivity. A careful study of this problem has been carried out by Folkmann et al.[44]). Their results for an energy of 3 MeV/amu are shown in fig. 8. It will be noted that for light elements all particles give the same sensitivity. The reason is that in this region the dominant background component is secondary bremsstrahlung. As discussed in section 4.1, production of characteristic X-rays and of secondary bremsstrahlung are closely related and for the same velocity both scale as Z^2. Hence, the ratio between the yields of the two processes does not depend on the choice of particle. For heavier elements heavy ions should in principle be superior, since they do not directly produce any bremsstrahlung (section 4.2). However, according to Folkmann et al., this advantage is off-set by a strong γ-ray background which gives an inferior sensitivity for α-particles and heavy ions. It can be seen in fig. 8 that even protons give rise to some γ-ray background, since the experimental curve lies above the calculated one. It should be kept in mind, however, that no systematic comparison as a function of excitation energy between different particles has been made. If the γ-ray background is so important, it might be worth while to try α-particles and heavy ions with somewhat lower energies than are commonly used. Recently Watson et al.[42]) have published some background spectra for various particles at 1.7 MeV/amu. They indicate that α-particles are superior to protons for some Z-values but since the spectra only cover the light element region it is difficult to draw any general conclusions.

From these considerations the best choice of excitation projectile appears to be 1-2 MeV protons. This conclusion is supported by the practical experience gained so far (discussed in section 8.1). This is, of course, rather fortunate since a small proton accelerator is cheap and easy to operate and there is a large number of such accelerators available. Since their usefulness for nuclear physics research is somewhat limited, it should be advantageous to use them for PIXE analysis.

With the above values for the experimental parameters, the minimum detectable concentration is found to be about 10^{-6}. However, as already explained these assumptions are rather conservative, corresponding to routine analysis. If it is desirable, one can with some effort improve the sensitivity considerably. Increasing the target thickness, the solid angle subtended by the detector and the collected charge about one order of magnitude, which should be within the reach of the experimental possibilities, gives according to eq. (6) an improvement in sensitivity by a factor of 30. Rather little has been done experimentally to push the sensitivity to its limit but already in the first publication on this subject it was shown that 4×10^{-11} g of Ti deposited on a thin carbon backing could easily be detected[1]). The values of target thickness and beam area were such that this corresponded to a concentration of 10^{-6}. The peak was well defined and the minimum detectable concentration can easily be calculated from the counting rates in the peak and in the background. It turns out to be 10^{-7}. This value is in good agreement with the results of the previous discussion showing that the calculated sensitivities agree well with the experimental possibilities.

Sensitivity can also be expressed as the minimum detectable absolute amount. This can be calculated from the concentration of an element if one knows the amount of sample material transversed by the particle beam. Here the situation can differ widely depending on what kind of material one is analysing. If enough material is available, as for example in air pollution studies, it is usually collected on a large, fairly thick backing. With a thickness of 10^{-4} g/cm^2 and an area of 1 cm^2, a minimum detectable concentration of 10^{-6} corresponds to 10^{-10} g. In analysing very small amounts of material one can without difficulties use a target thickness of 2×10^{-5} cm, a beam area of 1 mm^2 and push the minimum detectable concentration to 10^{-7}, which corresponds to 2×10^{-14} g. The ultimate lower limit in detectable amounts of material is obtained by the microprobe technique in which the particle beam is so well collimated that the fine structure of the sample can be studied with a scanning technique. Beam diameters of about 5×10^{-4} cm have been reported. A target thickness of 2×10^{-5} cm and a concentration of 10^{-5} then gives 5×10^{-17} g. Of course, these numbers are only meant as an illustration of the theoretical possibilities without consideration for the practical problems, but they clearly show that the PIXE technique allows detection and analysis of very small amounts of material.

A problem which should be mentioned in this connection is the introduction of impurities during the sample preparation. It is of little use to have an analysing method of high sensitivity if some trace elements in the material to be analysed are masked by impurities. The main problem here is the backing which must be used, for example, in the analysis of aerosols or solutions. The purity of the backing material is discussed in section 7.8.

Impurities can also be introduced during the handling of the sample. Even a short exposure to the atmosphere can cause problems. A single dust grain of medium size (1 μm) has a weight of about 10^{-12} g and a comparison with the numbers given above clearly shows that extreme caution must be exercised if the highest sensitivity is to be attained. This problem is also discussed in section 8.2.

6. Quantitative analysis

The basic formula used to calculate the amount of a certain element in a sample from the corresponding peak in the X-ray spectrum is the following

$$\mathrm{d}N = A(s)\, n(s)\, \sigma\omega k\Omega T\varepsilon\, \mathrm{d}S. \tag{7}$$

$A(s)$ is the number of atoms in a surface element $\mathrm{d}S$ of the sample, $\mathrm{d}N$ the number of counts due to these atoms, $n(s)$ the total number of protons per cm^2 passing through the same surface element, σ the cross sections for ionization of the corresponding shell, ω the fluorescence yield, k the relative transition probability for the particular X-ray transition used in the measurements, Ω the solid angle subtended by the detector, ε its efficiency and T the transmission through the window of the irradiation chamber. Included in T is also the self-absorption in the sample and the absorption in any absorber that might be used.

A discussion of this formula is very instructive and gives a background to the problems one encounters in applying PIXE to quantitative analytical work.

To get the total number of counts in a peak one has to integrate eq. (7) over the entire sample keeping in mind that both A and n are functions of the position s.

$$N = \sigma\omega k\Omega T\varepsilon \int_s A(s)\, n(s)\, \mathrm{d}S. \tag{8}$$

Evaluation of this integral requires knowledge of the beam profile and the matter distribution in the sample. However, the problem is very much simplified if the density distribution of the beam is rectangular, i.e. n is independent of s inside the beam and zero outside. Then

$$N = n\sigma\omega k\Omega T\varepsilon \int A(s)\, \mathrm{d}S = An\sigma\omega k\Omega t\varepsilon, \tag{9}$$

where A denotes the total number of atoms in the sample of the particular element to be determined.

The methods used to obtain a beam with a constant particle density over the whole beam area will be discussed in section 7.1.

The number of counts N in a peak is often determined manually by estimating and subtracting the background and adding the remaining counts in the peak. With many spectra each containing several peaks this is a tedious procedure. Therefore it is preferable to use a computer program which fits a Gaussian with exponential tails to each peak and a polynomial to the background. The details of this procedure will be discussed in section 7.6.

The proton flux, n, is determined by collecting the beam in a Faraday cup (section 7.1).

The quantities σ, ω and k have been discussed in section 3.1.

The solid angle subtended by the detector is determined by the geometry of the experimental set-up. Sometimes the size of the detector is not accurately known. It is also poorly defined due to the presence of an annular dead-layer. It might therefore be better to define the solid angle by a collimator in front of the detector.

The efficiency, ε, of the detector might be obtained from data provided by the manufacturer. In many cases the accuracy of such data is not sufficient and it is therefore advisable to calibrate the detector. This can be done by means of radioactive sources of known strength. A difficulty is that there are no suitable sources with energies below 6 keV. In order to determine the low energy part of the efficiency curve one can make use of eq. (9) and bombard thin foils of known thickness.

In determining the transmission T, the absorption of the X-ray in windows and absorbers does not present any problems. The main difficulty is self-absorption in the sample. Even in a relatively thin sample, for example 1 mg/cm^2, the X-rays from low-Z elements suffer considerable attenuation. In thicker samples, the calculation of the X-ray absorption is a major problem requiring knowledge of the composition of the sample as well as of any inhomogeneities. These problems are treated in section 7.9.

Implicit in the foregoing discussion has been the assumption that the cross section σ is constant. In thicker targets this is no longer true since the incident particles are slowed down. This is an important effect which has to be considered since the cross section depends so strongly on the energy. The special problems connected with thick targets will be discussed further later.

The above discussion shows that all quantities in eq. (7) except A and N either are known or can be experimentally determined. Hence PIXE is an absolute method. It is, of course, a great advantage not to have to rely upon standard samples or internal standards. Experience clearly shows that this is not only a theoretical possibility but something that can be realized in practical analytical work on a routine basis. This is further discussed in section 10.4.

It should be obvious that there are cases, especially with thick, non-homogeneous samples, where the various corrections needed are rather difficult to calculate and to apply. In such cases it might be advantageous to use an internal standard. Usually the sample to be analysed is doped with some suitable chemical compound in known concentration. Several elements have been suggested for this purpose.

Another possibility to facilitate the analysis of thick samples is the use of a standard sample of known composition. The standard sample and the sample to be analysed must contain similar relative amounts of major elements. Both samples are bombarded under identical conditions. A comparison of the peak heights in the two spectra obtained then directly gives the elemental abundances in the unknown sample. An example of the use of this method is the work of Clark et al.[46]) where basalt rock was analysed using a granite as a standard.

7. Experimental arrangements

7.1. Irradiation chamber

During the initial phase of PIXE development, workers used chambers otherwise designed for nuclear physics work. At the present moment, several laboratories operate fully or semi-automated systems including remotely controlled sample changing and on-line data reduction[47–53]).

A versatile and efficient chamber design should allow for rapid and sensitive analysis of many types of samples. Low background, a homogeneous beam of sufficient intensity, tight geometry and arrangements for sample and absorber changing are therefore needed. Fig. 9 illustrates the principles of a typical chamber design. Target changing may be done through a vacuum lock in order to maintain the chamber vacuum. The targets are often mounted on regular 50×50 mm^2 slide mounts and kept in slide trays typically holding about 35 samples. Target changing mechanisms are therefore often modified commercial slide changers.

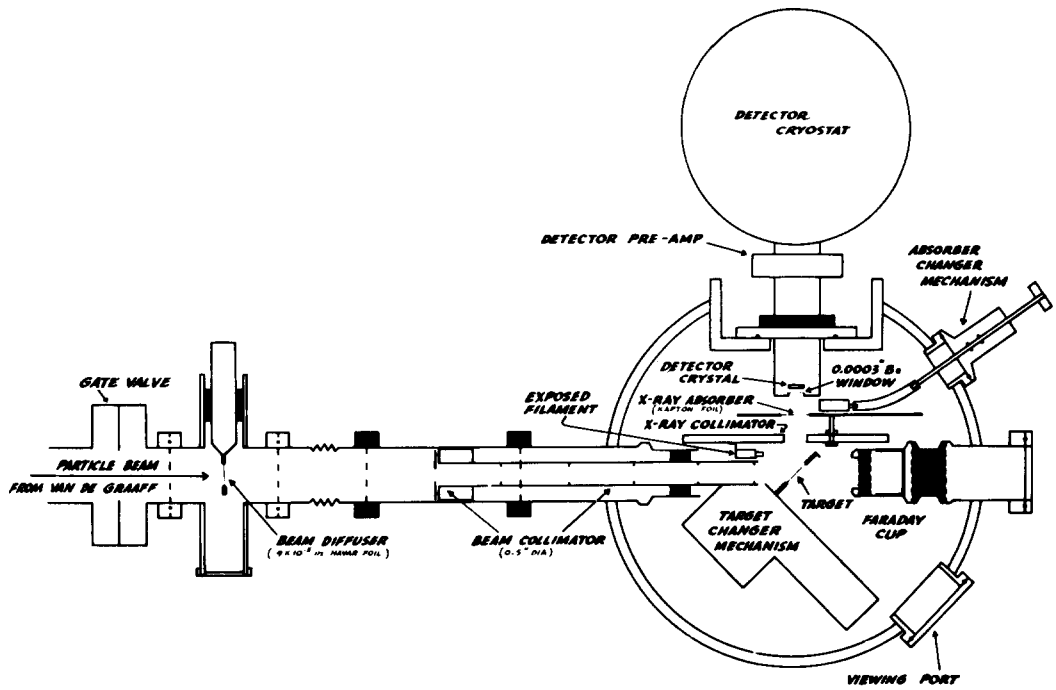

Fig. 9. A typical PIXE analysis chamber. From ref. 49.

For routine analysis this is a sufficient arrangement. It is often found that the possibility of being able to manipulate the target position in the beam is valuable. Micrometer screws are used in a simple holder arrangement fitting into a hole in the chamber wall with a small gear-rack included for movement.

For many applications, it is also very useful to detect other types of radiation from the target, including such charged particles as scattered protons and other nuclear reaction products. This may be done to determine more elements in the sample or simply to determine the amount of material analysed, about which the number of scattered particles gives information. A chamber should therefore be designed so that it is possible to incorporate detectors for these reaction products.

To reduce chamber background levels, it is important to use materials which give rise to negligible amounts of radiation when struck by a particle beam. Aluminium has been used extensively for this purpose and care has often been taken to find ultra pure aluminium for parts of the chamber. Aluminium has the advantage of low energy characteristic X-rays but the drawback of giving rise to an intense nuclear γ-radiation when stopping a proton beam. Herman et al.[54]) obtained significant background reduction by using an X-ray collimator of pure aluminium thereby eliminating X-rays generated by protons scattered from beam collimators and the target from being seen by the detector. This arrangement was also used by Stupin et al.[11]). Vis and Verheul[55]) lined all surfaces visible from the detector with teflon to avoid the production of characteristic X-rays of impurities in the aluminium by scattered electrons. Jundt et al.[56]) used a 2 mm thick polyethylene and Kubo[57]) a 1 mm polyvinyl sheet for the same purpose. The beam collimators themselves are a potential source of intense background radiation. This is often conveniently minimized by the use of carbon collimators combined with particle energies below 1.6 MeV for protons. The size of the beam is typically in the range of 1–10 mm diameter.

As mentioned above, the fundamental approach to quantitative analysis calls for a homogeneous beam. This has been achieved by sweeping[5]) a well-focused beam over the collimator entrance or by inserting a diffuser foil[10]) upstream to let the collimators select only a central fraction of the diffused beam. Bearse et al.[58]) defocused the beam while still within the accelerator and let the beam travel $\sim$8 m to the target area, thereby losing 40% of its intensity. They were able to get a 200 nA beam to the target area, sufficient for many types of analysis. Cahill[47]) uses magnetic sweeping of the beam. All these approaches work well and provide a sufficiently homogeneous beam. One

should check experimentally that the arrangement selected actually provides the beam desired. Fig. 10 shows an example of beam homogeneity. Of course, defocusing is a simple approach in all cases where it is possible. Of the others, a diffuser foil is the least complicated arrangement but requires sufficient initial beam to allow for the intensity reduction with a factor of 10-20. Great care must be given the choice of materials for diffusers and areas where 90-95% of the beam is dumped since this process takes place near the detector and could increase the background drastically. One arrangement is to place a well shielded 9 mg/cm^2 Al foil about 1 m from the target area. The slowing down of the protons will introduce some straggling but even with a foil as thick as 9 mg/cm^2, the error thus introduced in the quantitative analysis has been estimated to be less than 0.5% [51]). Although beam sweeping is less demanding in some respects, the equipment needed makes it more complicated unless beam deflecting arrangements for fast beam control have been included for other reasons. The importance of proper design of beam scatterers and dumps as well as the rest of the beam handling system is illustrated by the data of Herman et al.[54]) presented in fig. 11. For proper beam alignment, current-readable collimators are convenient. Careful design of the collimators may reduce slit scattering effects[59]) and thus chamber background.

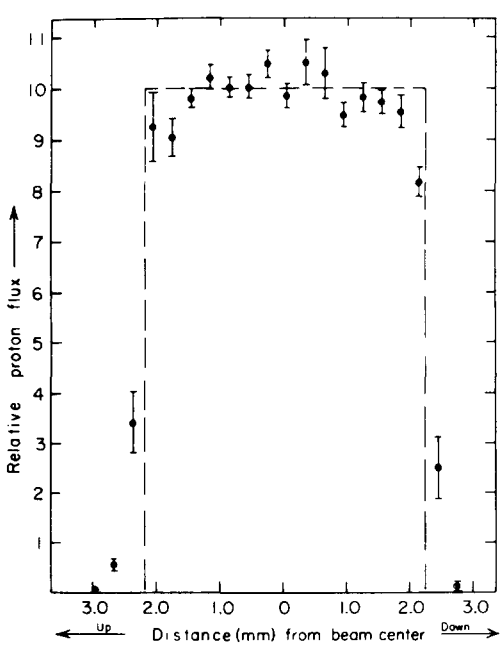

Fig. 10. Intensity distribution of a proton beam used for PIXE analysis. From ref. 51.

Most workers have placed the X-ray detector perpendicular to the particle beam and very close arrangements with sample-detector distances of only a few cm are in use. Feldt and Umbarger[60]), for example, report a distance of less than 2 cm. Other orientations of the detector have been discussed but abandoned on the grounds that the angular distributions of both characteristic and background X-ray production are too isotropic to be utilized for optimization. However, experimental data have only been available for characteristic X-ray production, where isotropy is good to a few per cent. Secondary electron background is less isotropic and recent measurements by Chu et al.[61]) indicate that a background reduction by a factor of two is possible by moving the detector to a backward angle (cf.fig. 12). In addition, a sample surface perpendicular to the sample-detector direction generally gives the smallest X-ray absorption in the sample. This is of critical importance for low-Z element analysis. Geometries with the detector in a backward angle are used by the Lund-FSU groups with the sample orientation depending on the application. The arrangement may introduce a small reduction in solid angle as the sample to detector distance is slightly increased.

A common experimental situation is that some low-Z elements, e.g. sulphur, are quite abundant in a sample also containing higher-Z elements of interest, or vice versa. In these cases, as well as those with a dominating bremsstrahlung background, the sensitivities for the elements of interest are reduced by the large count rate contribution from these sources and sensitivity improvements cannot be achieved by increasing beam intensity alone. Absorbers often help to improve the situation. Mylar films on the order of 10 mg/cm^2 are often used. In the case of abundant high-Z elements, the situation for some elements with lower Z is improved by using K-edge abosorption.

Unfortunately, however, the use of an absorber often eliminates or sharply reduces analytical sensitivity for a number of interesting trace elements.

A straightforward improvement is to allow for two or more irradiations of the sample using different absorbers and perhaps also different beam energies to emphasize the elemental region of interest. A more elegant approach is to use a small hole in the absorber[48]) to permit some soft X-rays to reach the detector, but with a smaller solid angle than the high energy X-rays. Fig. 13 shows the product of cross section for K_α lines, efficiency and solid angle for three configurations. For the same time and count-rate, the sensitivity for medium and heavy elements is improved

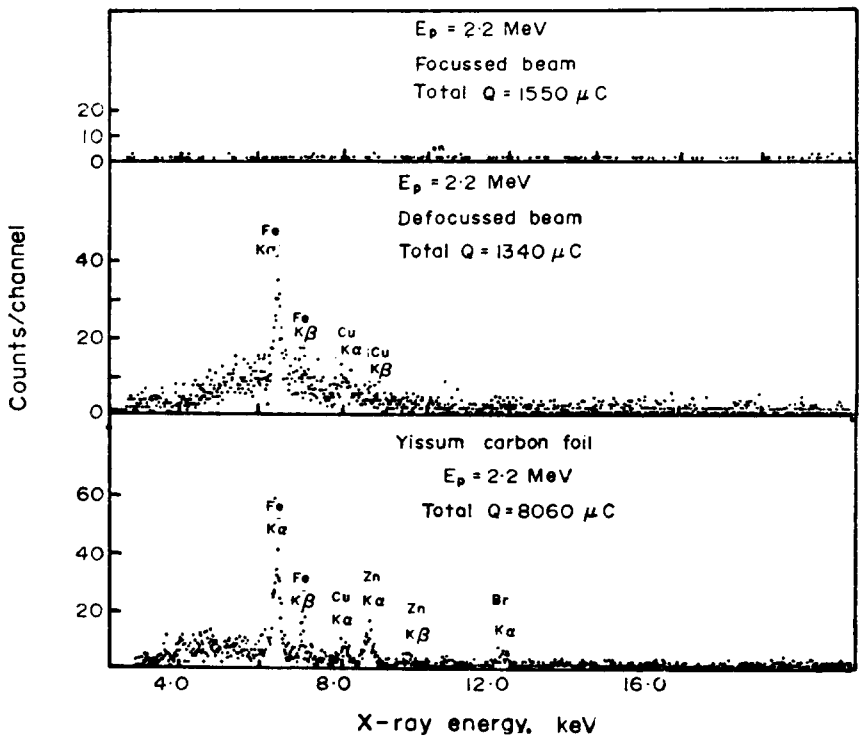

Fig. 11. Chamber background with a well focused beam is depicted in the upper part of the figure. In the middle is shown the increase in background caused by defocusing the beam. The lower part of the figure shows the background originating in the carbon backing. From ref. 54.

three-fold with this arrangement. For convenience, a remotely controlled absorber selection is a good arrangement.

Beam charge measurements are generally carried out by charge integration from a Faraday cup. The target may be enclosed in thin target work and is always enclosed in thick target arrangements. Electron suppression is sometimes included, but, for thin target work, its effect is not more than a few per cent. For very tight designs with surfaces not included in the Faraday cup although in the vicinity of the beam, the effect may be much larger. For work with insulating targets, arrangements to prevent charging of the

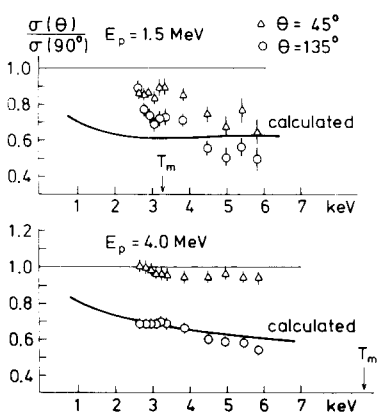

Fig. 12. Ratios of bremsstrahlung production cross sections measured at 45° and 135° to those at 90° obtained with proton beams of 1.5 and 4 MeV. From ref. 61.

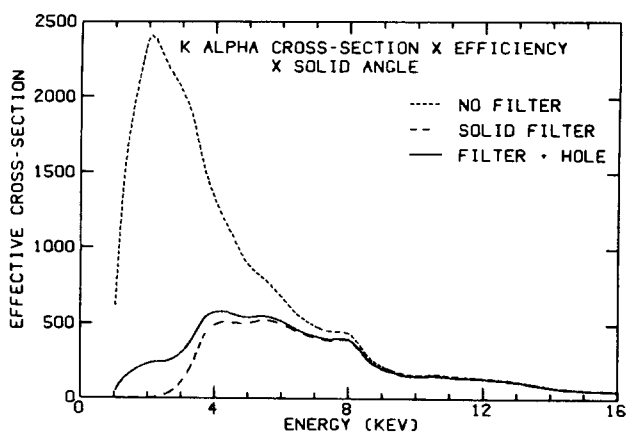

Fig. 13. Effective cross section of K_α lines for an absorber having a small hole. The absorber material is 30 mg/cm² Kapton. The area of the hole is 0.1 times that of the detector. From ref. 48.

target are needed. The target can be sprayed with electrons[62,63]) or the chamber can be operated under slightly higher pressure than normal[63]). Fig. 14 shows an arrangement of electron gun and electronic coupling which permits simultaneous accurate beam charge integration.

Cold traps have been included in some arrangements[1,54]) to condense any vapours in the chamber which might contaminate the sample. Experience in our laboratory indicates that contamination by heavy elements without a cold trap is generally negligible. Results by Khan et al.[64]) suggest that the condensed material on the sample is to better than 90% carbon, a result supported by Quaglia and Weber[65]), while Bales et al.[66]) did not observe any build-up using 100 keV protons to get 1.2 mC charge. They conclude that build-up on the target is important only when very low proton energies are used.

Most systems operate under moderately high vacuum, 10^{-5}–10^{-6} torr. Both oil and mercury diffusion pumps are used; no target contamination problems have been observed with mercury pumps probably due to the revapourization of any mercury condensed on the target. Beezhold[67]) has described a chamber for ultra-high vacuum needed for studies of implantation and analysis. He reaches 10^{-10} torr using vac-ion-pumps, metal seals and four different pumping regions separated by constrictions. Beezhold's chamber also has facilities for target manipulation capable of positioning samples for channeling studies as well as in situ heating to 1200°C or liquid nitrogen cooling to 110°K. Another interesting feature of this design is an arrangement for use of a windowless detector for low-Z element analysis. An internal poppet valve separated the Si(Li) detector from the target area to permit sample changing at atmospheric pressure.

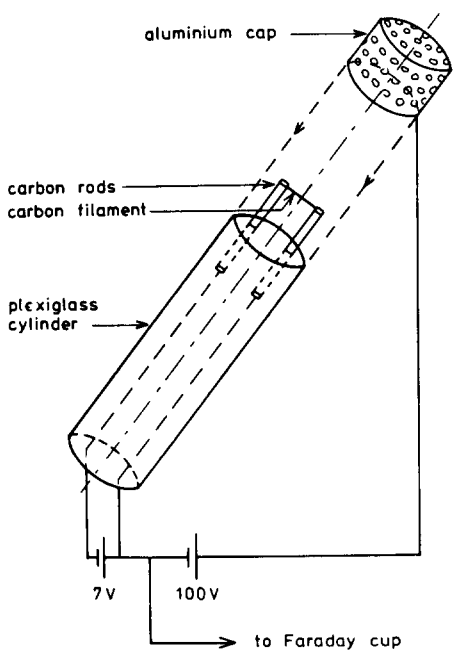

Fig. 14. Electron gun for spraying the target with electrons in order to prevent charging. From ref. 63.

7.2. External beam

The normal method of placing the sample in an evacuated irradiation chamber has some disadvantages, the main one being target preparation. Liquid samples have to be evaporated to dryness and samples containing water, for example, organic tissue, deteriorate in vacuum. A solution to these problems might be to use an external beam and several attempts to explore this technique have been made.

Deconninck[6]) used an arrangement in which the proton beam passed out through a nickel foil and entered an irradiation chamber filled with helium at atmospheric pressure. Used lubrication oil was analysed by this method.

Grönvall[68]) used an external beam for the analysis of water solutions. The beam passed out of the beam tube through a thin Kapton foil, which was simultaneously part of a small sample container for liquids. Hence the beam was stopped in the liquid. Sensitivities in the range $(0.1\text{–}1) \times 10^{-6}$ were obtained.

Seaman and Shane[69]) studied samples of wheat flour by means of an external beam. Mylar or nickel were used as exit foils for the beam. Mylar with a thickness of 13 μm could withstand a current of 10 nA and 0.13 μm nickel foils 30 nA. A disadvantage of the latter was the intense X-radiation produced in the foil, part of which was scattered by the sample into the detector.

The great advantage of an external beam is the simplified sample preparation and handling. Any type of sample can be irradiated directly and sample changing is easy. A further advantage is that the sample is more effectively cooled at atmospheric pressure than in vacuum. A complicating factor is the strong argon peak which appears in the spectrum when the beam passes through air. This can be avoided by surrounding the beam by a helium or nitrogen atmosphere. The measurement of the beam current is more complicated in the case of an external beam.

So far, experience with the external beam technique is rather limited and it is hard to judge if the obvious

advantages can compensate for the experimental complications.

A special case of an external beam is the microbeam of Horowitz and Grodzins[70]) described in the next section.

7.3. Microprobe

The electron microprobe offers a very powerful method for the analysis of microstructures. The limitation is the strong bremsstrahlung background from the electrons. This gives a rather poor sensitivity, of the order of $1:10^4$, so that only the major constituents of the sample can be determined. An obvious way to improve this situation is to replace the electrons by protons. However, it is far more difficult to focus protons than electrons and the development of the proton probe has therefore been rather slow. Beams with a diameter of about 0.05 mm have been used by several workers for microanalysis by means of nuclear reactions. Pierce et al.[71]) used a series of collimators to obtain a 0.025 mm beam which they then used for analysis by means of the γ-radiation emitted in inelastic scattering. Poole and Shaw[72]) used a 0.1 mm beam in combination with a crystal spectrometer. They recorded X-ray peaks for several elements but the sensitivity was poor because of background problems. A major improvement in beam focusing was achieved by Cookson and Pilling[73]) by using a series of quadrupole magnets. A beam diameter as small as 4 μm was obtained. Peisach et al.[74]) combined a beam of this type with the use of a silicon detector and demonstrated the possibility of analysing the microstructure of the sample by scanning the beam over its surface. Cho et al.[75]) have reported a theoretical and experimental study of beam focusing by means of two quadrupole doublets.

Horowitz and Grodzins[70]) used a very simple arrangement to produce a narrow beam. Protons from a van de Graaff generator passed through a small pinhole in a thin window at the end of the beam tube. The resultant pencil beam scanned mechanically over the sample. The X-ray signals from a silicon detector were used to construct a two dimensional picture of the sample for each element. In some preliminary experiments a 25 μm beam was used but it is claimed that a resolution of $\leqslant 1$ μm should be obtainable. The special problems and advantages connected with the use of an external beam are discussed in the previous section.

7.4. X-ray detection

Basically two principles of detection are available: energy- or wavelength-dispersion. Energy-dispersion detectors record photons of any X-ray energy and yield spectra of the type shown in fig. 2. Lithium-drifted silicon detectors are in widespread use and have typically a resolution of 150–180 eV with 30 mm^2 detector area. The large area and the capability of counting all energies without resetting allows for fast and efficient data accumulation. Energy-dispersion detectors have recently been reviewed by Goulding and Jaklevic[76]) and techniques of wavelength dispersion by Liebhafsky et al.[77]). Wavelength-dispersion systems operate with much smaller solid angles and internal efficiency. A scan procedure is necessary as the wavelength interval recorded is quite narrow. On the other hand, the resolution is of the order of tens of eV, a very attractive feature of these systems.

Wavelength dispersion detectors have not only been used for elemental but also for chemical state determinations (section 10.6).

The optimum choice of detector depends on the particular analytical task. The excellent resolution of wavelength dispersion detectors offers the capability of almost interference-free spectrum evaluation, while the broad peaks of energy-dispersion detectors commonly overlap and may, in complicated cases, make quantitative analysis dubious and even qualitative analysis unreliable. In these cases the MDL increases drastically due to interference counts in respective channels. Energy-dispersion systems on the other hand are fast and convenient. In many analytical situations the interference problems with energy-dispersion systems are not significant and the ease of using these systems has motivated their widespread use. For analytical PIXE work they have been used almost exclusively to date.

The large solid angle and high internal efficiency of energy-dispersion detectors permit the use of low intensity sources compared with wavelength dispersion detectors. For trace analysis this is a distinct advantage, since very weak signals can be detected if the background is low as in PIXE analysis. These same detector characteristics in other analytical situations may suggest the use of wavelength dispersion detectors. For example, when X-ray excitation is used, the exiting radiation scattered in the sample takes up a major fraction of the count-rate capability of the detector system. In such cases, wavelength dispersion detectors have much larger data accumulation capability but require more intense X-ray generation for efficiency reasons.

Several comparisons between wavelength-dispersion and energy-dispersion detectors using X-ray for

electron excitation have been published[78–81]). The MDL of the two systems compared are found to be of the same order of magnitude for multielement analysis situations. It is also found that wavelength dispersion detectors offer much better analytical precision, typically limiting the use of energy-dispersion detectors to situations for which a precision of several percent or more is sufficient.

The wavelength dispersion detectors are generally used with high-powered X-ray tubes, compensating for the low detector efficiency.

For PIXE work, energy-dispersion detectors with sufficient resolution for spectrum evaluation have proved to be very useful in most analytical situations. A few interference problems are however difficult: the Ba–Ti, K–Cd and Pb–S are prime examples. These can be handled in various ways. There is no doubt that the combined use of wavelength- and energy-dispersion detectors for this type of problems would be very beneficial and provide the information needed for reliable energy dispersion spectrum evaluation.

Such a detector combination would make use of the best characteristics of both systems. The data presented by Dewolfs et al.[79]), where 10 s wavelength-dispersion and 1000 s energy-dispersion detection with roughly identical excitation power gives similar MDL and rough calculations[82]) suggest that wavelength- dispersion detectors may be successfully used in this way.

The detector efficiency varies with X-ray energy and is at low energies limited by X-ray absorption in various windows and at high energies by penetration through the crystal. The detector efficiency need not be determined explicitly unless the fundamental approach to quantitative analysis is chosen. Efficiency information as supplied by manufacturers is only an estimate[83]) as it is solely based on calculation. Experimental efficiency determination is usually carried out using calibrated X-ray sources[84]). For low energy X-rays, this technique is limited by the lack of suitable sources. As this is in a region where efficiency varies rapidly with energy, other methods are needed. One approach[51]) is to use thin films of well-known composition and then determine the efficiency via eq. (9). In these experimental determinations it is often sufficient to calibrate the product of efficiency and detector area.

7.5. Electronics

The power of solid state detectors is dependent on the associated electronics. Elaborate designs have been developed to make full use of the potentialities of the detectors in processing the information in a flow of X-ray photons to a memory for subsequent evaluation. Typically, the charge pulse from the detector is converted to a voltage pulse using a cooled FET transistor in a preamplifier. To maintain the dc level, either a resistor feedback or pulsed optical feedback is employed. A main amplifier adjusts the signal to the requirements of an analog-to-digital-converter (ADC), which is the entrance module of a multichannel analyser of a computer-based data acqusition system. Modern amplifiers are equipped to handle high counting rates and the components are well developed. A recent discussion of the present state of the art has been given by Woldseth[85]).

Important problems are the handling of pile-up events and dead-time corrections. Woldseth discusses the performance of frequently employed circuits. Campbell et al.[86]) give an illustration of the pile-up problem in PIXE work. The modules used were originally developed for use in X-ray excitation analysis. Such work includes the processing of large numbers of high energy photons scattered in the sample while PIXE, on the other hand, is characterized by the absence of such pulses but with abundant low energy photons. In some applications the latter may of course be removed by an absorber. The solutions to the pile-up and dead-time correction problem in X-ray excitation work are therefore not necessarily directly transferable to PIXE as is indicated by the low count rates, on the order of 1 kHz, typically reported.

An alternative method for handling these problems has been suggested by Jaklevic[87]) who uses an excitation source with a pulse leading-edge sensor in the amplifier which triggers a turn-off of the excitation source during the processing of a pulse. The periodic pulse train created by this arrangement leads to an improvement of the system performance. It should be noted that this principle also permits effective dead-time correction.

Thibeau et al.[88]) have built a similar system for PIXE work and Cahill[47]) reports very good performance. The design must be based on deflection of the accelerated beam since the delays involved with ion-source controls are too long. Electrostatic deflection, therefore, is employed. Cahill also mentions that, with extensive modifications, a commercial dead-time circuit permits reliable operation.

Deflection of the particle beam has the advantage of reducing sample damage and chamber background. The reduced irradiation of the sample also means that the sample may be analysed at a higher effective beam-level, thus reducing the total time required for the analysis. The use of deflector plates may be coupled

with beam sweeping as discussed above or with beam scanning arrangements that may be designed for spatial resolution studies.

7.6. Spectrum analysis

To determine what elements are detected in a single run, their amounts and upper limits for other elements, it is necessary to locate and determine energies and intensities of all peaks in the X-ray spectrum. When only a few elements, well separated in energy, are present this presents no difficulties. However, in many applications multiplets of varying complexity must be resolved; this often constitutes a major problem in PIXE analysis. We would like to stress the importance of reliable and fast computer codes for all routine work with this analytical method, especially as very large numbers of samples must often be processed.

An approach taken by many has been to adapt computer codes originally designed for γ-ray spectroscopy to X-ray spectrum evaluation. One of the codes used in this way is SAMPO[89]) which has been used in many laboratories. Gaussian functions and a polynomial background are fitted over regions including up to six peaks at a time and give good results if carefully done. The code, however, requires rather large manual intervention, and it is therefore less suited for routine work. Similar approaches to the analysis problem have been taken by Jundt et al.[56]), Valkovic et al.[90]) and Stupin et al.[11]). All of them fit Gaussian functions on polynomial backgrounds. J.P. Thomas[91]) and Campbell[86]) subtract the background before deconvolution of overlapping peaks. Bearse et al.[58]), in their study of whole blood analysis, use a simpler approach. They add all channels in the region of interest and perform a linear interpolation for background estimation. They report Fe, Cu, Zn, Se and Rb quantitatively using Pd as an internal standard and find K, Ca and Ti qualitatively. In their specta this procedure works well with the exception for Cu, which is often a weak peak close to Zn K_α.

Automatic computer-controlled data acquisition is used in the system described by Harrison and Eldred[48]). During the accumulation of one spectrum, the previously-recorded spectrum is analysed in their PDP 15/40 computer. A total spectrum analysis using their specially written code takes about 90 s and the core required is as little as 9 k. This includes the acquisition routines but not input-output handling or the operative system. Harrison and Eldred first subtract the background using a previously recorded substrate without loading, in order to improve the speed and reliability of the peak search routine. For heavily loaded samples, the background contribution from the sample itself is not negligible and a separate subtraction procedure is used for this. Peak search is done with a Gaussian cross-correlation technique using two different widths (W) to be able to locate small peaks close to larger ones. Peaks are treated as multiplets if closer than $2W$ and then fitted to Gaussian curves, varying position, width and area. Corresponding elements are identified from a library and amounts determined using previously recorded calibration information. The accuracy of the peak position determined was found to be as good as 12 eV with this code.

Kaufmann and Akselsson[92]) have taken a different approach in their design of a special code for PIXE spectrum analysis. They make maximum use of the physics involved in the X-ray generation and detection and arrive at a functional model describing the spectrum as a function of a number of parameters. This model is then minimized using a new minimization routine developed for the task. Their code presently requires a few minutes of computer time and resides in a 24 k memory. The functional model, $f(P, E)$, where P stands for all parameters to be determined and E is the X-ray energy, is made up of two parts, one describing the background and one the X-ray peaks. The background originates from bremsstrahlung emitted from secondary electrons ejected by the particles when passing through the target. This mechanism dominates the low energy part of the spectrum while in the high energy part the background is generated by

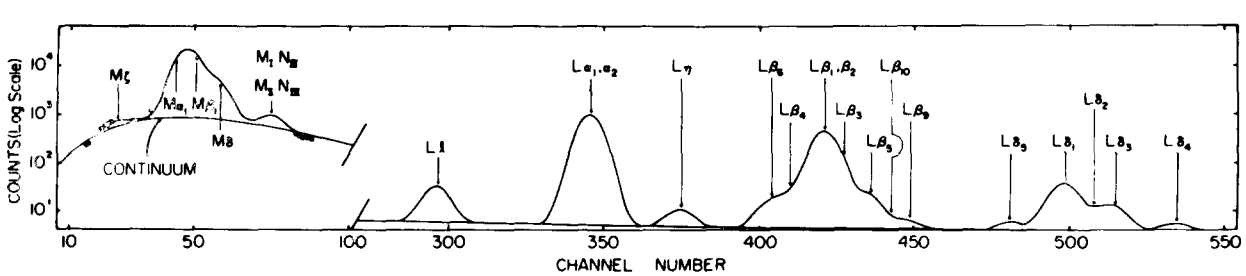

Fig. 15. A pulse height spectrum from PIXE analysis of a lead foil. From ref. 92.

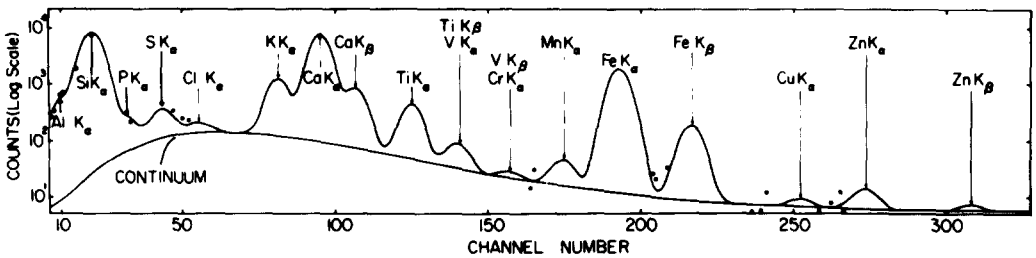

Fig. 16. An aerosol spectrum analyzed by the code of Kaufmann and Akselsson. Points deviating more than two standard deviations are plotted. From ref. 92.

Compton scattering of X-rays and particle bremsstrahlung. These contributions are described with exponential functions and multiplied with appropriate X-ray absorption functions. The second part of the model is a sum of all X-ray peaks from elements included in a library. Each peak is described as a Gaussian distribution, with a width depending on its energy. Several peaks with fixed intensity ratios are included for each element. For example, the lead spectrum consists of as many as 23 components (cf. fig. 15). Each Gaussian is then multiplied by the appropriate X-ray absorption function. Altogether, the number of parameters used is one for each element included plus 12, the latter covering background and energy calibration. Fig. 16 shows the results of the analysis of an aerosol spectrum with this code.

The important feature of the last two codes described is, which should be emphazised, to permit the processing of large numbers of spectra without operator intervention.

7.7. Interferences

The large number of X-ray lines and the limited resolution power of Si(Li)-detectors makes line interferences unavoidable. Fortunately, in most analytical situations there are methods to handle these problems. In the computer code for spectrum evaluation by Kaufmann and Akselsson discussed above, interferences are handled intrinsically in the code, a nice consequence of their approach. For other spectrum evaluation methods, line-interference corrections must be made after peak locations and areas have been determined.

A frequently encountered interference problem is that between K_α of element Z and K_β of element Z-1. This interference occurs in the transition region where the detector resolution separates K_α from K_β for element Z. For higher-Z elements, the energy differences permit the detectors to separate these interfering lines. From Z values around 35 and up, the interferences between L-lines from these elements and K-lines from lighter elements have to be considered. For elements in the lead region interference between M-lines from these elements and K-lines from elements in the sulphur region occurs. Table 5 gives some examples of X-ray interferences of these types. Bearden's[93]) very useful list of X-ray energies helps identify possible interferences. Whether or not all these possible interferences will be of practical importance is a question of relative elemental abundances and analytical sensitivity. In typical applications, not more than 10–15 elements are detected so interference problems are rather limited and methods to cope with them exist in most cases.

As the relative K-line intensity from one element is constant no matter whether excited by photons, electrons, protons or alphas, we may use

Table 5

Examples of X-ray interferences. Line energies from ref. 93.

Lines	keV	Difference (eV)
Mo $L_{\alpha 1}$	2.293	
S K_α	2.308	15
Pb $M_{\alpha 1}$	2.346	38
Pb M_β	2.443	97
Cd $L_{\alpha 1}$	3.134	
K $K_{\alpha 1}$	3.314	180
Cd $L_{\beta 1}$	3.317	3
Ba $L_{\alpha 1}$	4.466	
Ti $K_{\alpha 1}$	4.511	45
Ba $L_{\beta 1}$	4.828	
Ti $K_{\beta 1}$	4.932	104
V K_α	4.952	20
Pb $L_{\alpha 1}$	10.552	
As $K_{\alpha 1}$	10.544	8

uninterfered lines for successive unravelling of the spectrum. This works well for K_α–K_β resolutions but calibration experiments are needed for determining the magnitude of L- and M-lines when their respective K- or L-lines are detected. However, as the X-ray production cross sections are larger for M-lines than for L-lines which are in turn larger than for K-lines, the uncertainty of detected elements increases if possible interferences cannot be corrected for or estimated due to undetectable K- or L-line interference. In such situations, as well as when several elements contribute to the counts recorded in an X-ray channel, information from crystal diffraction experiments could give accurate information on one or two lines and thus help resolve these interferences. For aerosol analysis, Ba–Ti and Pb–S interferences are the most difficult to handle. Harrison and Eldred, in their code, reach a level of accuracy in peak location determinations which helps them to resolve the Ba–Ti interference with the help of relative line intensities.

7.8. Backing material

Several considerations may guide the choice of backing material for PIXE analysis. The backing must consist of low-Z material and contain minimal amounts of higher-Z impurities in order to avoid peak interferences for the elements to be analysed. Also, backings ought to be thin to minimize the X-ray background and thus increase sensitivity. Finally, the strength of the backing is of prime importance for its ability to withstand irradiation, handling, and target preparation procedures. Many materials have been used for backings. Table 6 presents some information on commonly used materials. The optimum choice depends on the analytical situation as all parameters cannot be optimized simultaneously. For example, carbon foils withstand very intense beams and are thus excellent for the analysis of very small amounts but are fragile and are less suited for work involving great numbers of samples or extensive sample handling. The advantage of a thin backing with associated low bremsstrahlung

Table 6

Characteristic properties of some commonly used backing material. More detailed information can be found in the references.

	Thickness $\mu g/cm^2$	Performance in beam	Impurities	Mechanical strength	Comments
Carbon[1,5,94])	20	μA, hours	Fe, Ni, Cu, Zn (Cl, Ca) [~0.1–1 ng/cm^2 [94])]	fragile	
Collodion[57])	<1 μm	5 nA/cm^2 30 nA/cm^2, 30 min if sandwiched	—	strong	Easy to handle; the low beam capacity has been improved by evaporating carbon or aluminum onto the film.
Formvar	10 ~50 100 aluminium	200 nA [58]) 3 MeV, 300 nA 500 s [90])	Fe, Cu, Zn (~ng/cm^2) [52])	fragile	
Kapton[95])	20	>300 nA	K, Ca, Ti, Cr Mn, Fe, Ni, Cu, Zn (~ng/cm^2)	fragile	Preparation similar to polystyrene, see ref. 51. Difficult to float off and handle. Impurities level probably not inherent in material and may be reduced.
Millipore	~5000	300 nA/cm^2	—	strong	
Mylar	500			very strong	
Nuclepore	~1000	300 nA/cm^2	Mn, Fe, Ni, Cu, Zn (~ng/cm^2) [52])	strong	
Polystyrene[51])	40	100 nA	Ca, S, Mn, Fe, Zn (~ng/cm^2)	strong	Preparation described in ref. 51.

background can be kept by using polystyrene or formvar foils. These foils are mechanically stronger than carbon foils but tolerate less beam. Mylar and commercial kapton films are very strong but also much thicker. Comparisons in this laboratory indicate[95]) that the bremsstrahlung increases with a factor of 15 in regions of interest and thus the lower limit of detection will increase by a factor of about 4. A more detailed study of sensitivity as a function of target thickness in the range 700–8000 $\mu g/cm^2$ has been published by Flocchini et al.[3]). The conditions of the analytical situation will determine whether a loss of sensitivity is an acceptable price for increased ease of handling. In table 6 we have included also Nuclepore and Millipore filters. Use of filters is often advantageous as further sample handling is not needed and contamination risks are thus minimized. These filters are now being used as backing substrates in several laboratories, even in cases where the sample cannot be collected on the filter directly. Other filters used in this way include Whatman (8 mg/cm^2) but their thickness and/or trace element content make them less ideal both for sensitivity reasons and for increased sensitivity to beam heating.

7.9. Target preparation

Target preparation is one of the central problems of PIXE analysis. The simplest case is the direct bombardment of a specimen. This method is often used for such materials as certain biological tissues, e.g. teeth, or metallurgical samples, where it is difficult or impossible to obtain thin targets. The drawbacks, mainly the lower sensitivity and the need for various corrections in calculating the results, are disussed in section 10.4

In most cases it is preferable to use thin targets. The material to be analysed is deposited on some suitable backing. There exists a great number of methods for bringing a sample into a form suitable for analysis and for depositing it on the backing. The method chosen depends on the type of material to be analysed. The most common type of samples are described in section 10, where the practical applications of PIXE are discussed. It is natural to discuss the target preparation technique in this connection.

7.10. Absorption in the sample

The sample itself may affect the accuracy of an analysis in two ways. The protons are slowed down when penetrating the sample material, thus changing the cross section for X-ray production and the X-rays induced are absorbed in the sample material. For thick target analysis, the protons come to a complete stop and an integration is performed to account for the distribution of the X-rays produced and their respective absorption in the sample.

In thin target analysis, the proton energy is reduced during the passage through the sample. For sample thicknesses of a few mg/cm^2, this is typically an effect of a few per cent. It can easily be corrected for by using an average proton energy, since the energy dependence of the cross section is a rather slowly varying function.

The absorption of the X-rays in the sample present a more serious problem. Fig. 17 illustrates the corrections that have to be made. As can be seen from the figure keeping below about 1 mg/cm^2 may limit the corrections to the order of 20% or less. Sometimes, this cannot be achieved and a proper evaluation of the absorption must be carried out. For homogeneous targets, where homogeneous X-ray production can be assumed, the correction is straightforward and given by the expression

$$t = \frac{1}{\mu d/\sin\varphi}\,(1 - e^{\mu d/\sin\varphi}), \tag{10}$$

where d is the thickness of the sample in g/cm^2, φ the angle between the sample normal and the beam and μ the mass absorption coefficient. This holds for an experimental geometry with the detector perpendicular to the proton beam. By changing this angle and the angle φ, absorption problems can be reduced.

The relative importance of the corrections for proton energy loss and X-ray absorption is shown in fig. 18 [Nielsen et al.[96]].

In many applications, particle size effects on the X-ray absorption must be taken into account. Rhodes

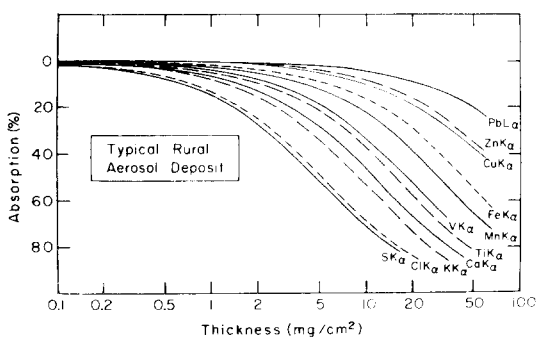

Fig. 17. X-ray attenuation in a homogeneous sample as a function of sample thickness. The calculations have been performed for a model aerosol consisting of 76% C, 9% O, 2% Al, 4.2% Si, 5% S, 2.9% Ca and 0.9% Fe. From ref. 51.

and Hunter[97]) have derived a set of simplified formulas for the practical cases of "thin" specimens, monolayers and samples with low or high packing fractions In the case of aerosol analysis particle size effects must be considered, especially when analysing elements with Z below about 20. Giauque et al.[98]) have developed an approach for X-ray excitation analysis utilizing two different X-ray energies for the excitation. Dzubay and Nelson[99]) use a dichotomous sampler that separates particles into two size-fractions with a cut-off diameter of about 2 μm. They treat the fine-particle fraction as a monolayer with an exponentially decreasing depth profile in the membrane filter and the coarse particle fraction as spherical particles. Cascade impactors are widely used for aerosol collection and provide particle size fractionated samples. This facilitates the X-ray absorption correction but, if long sampling times are used, the shape of the aerosol deposit under the jet introduces additional problems and can decrease the precision. When samples are collected on filters, some penetration of the particles complicates the evaluation as filter material absorption has to be considered. Adams and Van Grieken[100]) have treated this situation and suggest folding of the filter prior to analysis to simplify the correction.

8. Practical considerations

8.1. Sensitivity

An important problem is the optimization of the experimental set-up for maximum sensitivity. There are a number of parameters such as bombarding energy, particle type, beam current, measuring time, etc., which have to be chosen rather carefully if optimum conditions are to be obtained. This choice is limited, however, by certain restrictions. For example, the measuring time cannot be made too long for practical reasons and the usable beam current is limited by the deterioration of the target. These problems will now be discussed in more detail.

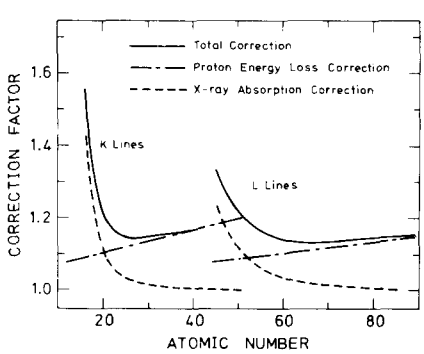

Fig. 18. Correction factors for a Nuclepore filter of 1.0 mg/cm² thickness. From ref. 96.

In section 5 we have shown theoretical curves for the sensitivity (or more exactly the minimum detectable concentration) as a function of the atomic number for different bombarding energies. It is evident that for each part of the periodic table there exists an optimum energy. In principle one should therefore adjust the energy according to which element one wants to determine in order to obtain maximum sensitivity. Such an adjustement would, of course, throw away one of the great advantages of the present method, its multielemental character. Hence, in practice, one has to choose the bombarding energy which gives the best overall sensitivity. In doing so one has to know which parts of the periodic table to emphasize. The following trace elements are often found in biological and environmental samples: Ti, Cr, Mn, Fe, Ni, Cu, Zn, As, Br, Sr, Rb, Zr, Mo, Cd, Hg, Pb and U. Hence the main interest ought to be concentrated to the two regions: $20<Z<40$ and $75<Z<92$. In order to give a clear picture of how the sensitivity varies as a function of bombarding energy and atomic number, fig. 19 has been prepared. It exhibits the minimum detectable concentration as a contour plot and has been calculated in the same way as fig. 7. It is obvious that if one wants to emphasize the regions mentioned above the optimum energy is about 2 MeV. It is a fortunate coincidence that both the medium and the heavy mass region can be optimized with the same choice of bombarding energy. It will be noted that for this energy the sensitivity does not deviate from the mean value by more than a factor of 2–3 in either direction. Such a constancy in sensitivity over practically the entire periodic system is, of course, a great advantage in analytical work. The low value of the optimum bombarding energy is another fortunate circumstance. Small accelerators capable of delivering 2 MeV protons are rather numerous. Since their price is relatively low, it is even quite conceivable to install such an accelerator for analytical applications. Economical aspects will be discussed further in section 12.

A similar calculation can be performed for α-particles. On general grounds one would expect optimum conditions for α-particles with the same velocity as 2 MeV protons, i.e. having an energy of 8 MeV.

It was shown in section 5 that the minimum detectable concentration scales as

$$\Delta E^{\frac{1}{2}}(\Omega j t)^{-\frac{1}{2}}. \qquad (6)$$

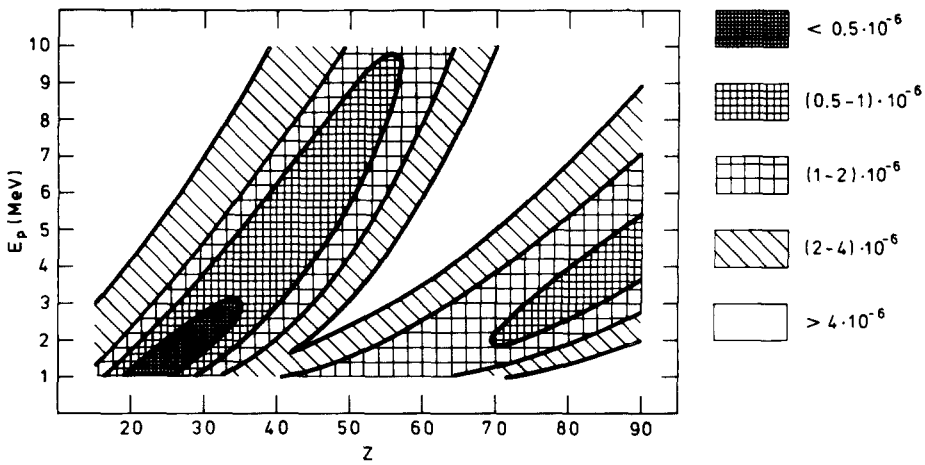

Fig. 19. Minimum detectable concentration as a function of atomic number and bombarding energy. The experimental parameters are the same as in fig. 7.

This expression guides the optimization of the experimental conditions.

The resolution of the detector ΔE is more or less fixed and hence of no interest in this connection.

The thickness of the target t should obviously be as large as possible. There are, however, certain limitations. An increase of the thickness can lead to excessive heating and deterioration of the target. Furthermore, it is desirable to have the target so thin that the slowing-down of the protons and the absorption of the X-rays can be neglected. Otherwise it is necessary to apply fairly large and uncertain corrections. This can be a complicated and tedious process as discussed above. Other limitations are the availability of target materials and the technical difficulties of preparing thick targets of some materials. Hence, in general the target thickness is determined by so many considerations that it cannot be regarded as a free parameter in the optimization of the sensitivity.

The solid angle subtended by the detector Ω ought to be as large as possible. The only limitations are the geometries of the irradiation chamber and the detector.

The collected charge j must also be maximized for optimum sensitivity. This can be done in two ways. One is to increase the measuring time. A rather normal choice is 5–10 min. It is obvious that in order to increase the sensitivity substantially, say by a factor of 3, one comes to measuring times which are impractically long. Hence not so much can be gained in this way. The other possibility is to increase the beam current. Here we have the limitation that a high current might cause excessive heating and deterioration of the target. However, as discussed in section 7.8, it is possible to prepare samples which are quite durable. Even organic materials have been shown to withstand appreciable currents. A great deal can be gained in sensitivity by using a high current and it is therefore important to develop target preparation techniques which make this possible.

As one tries to maximize the sensitivity in this way another difficulty may be encountered. The scaling law eq. (6) is only valid if there are no limitations to the counting rate in the detector. In practice, this is unfortunately not the case. The time constant of the pulses from a silicon detector is relatively long and high counting-rates can cause serious pile-up effects. A rather normal counting rate limit is 10 000 counts/s. Actually, at the present state of the art, it is the acceptable counting rate which in most cases determines the sensitivity. Ways of improving this situation are discussed in section 7.5.

A related problem is how to make the maximum use of the information in a spectrum. In a typical spectrum, for example the one depicted in fig. 2, a major part of the pulses go into the high peaks of some light elements such as Si, K and Ca. Furthermore, the background peaks at low X-ray energies. This means that the low-energy end of the spectrum takes up a great part of the available counting rate while giving little useful information. An obvious way to improve this situation is to cut down this part of the spectrum by a suitable absorber. This is now a common practice.

A more difficult case is that of samples containing a medium heavy element as a main constituent. Examples are steel and other metallurgical samples or semiconducting materials like Si and Ge. One possibility of

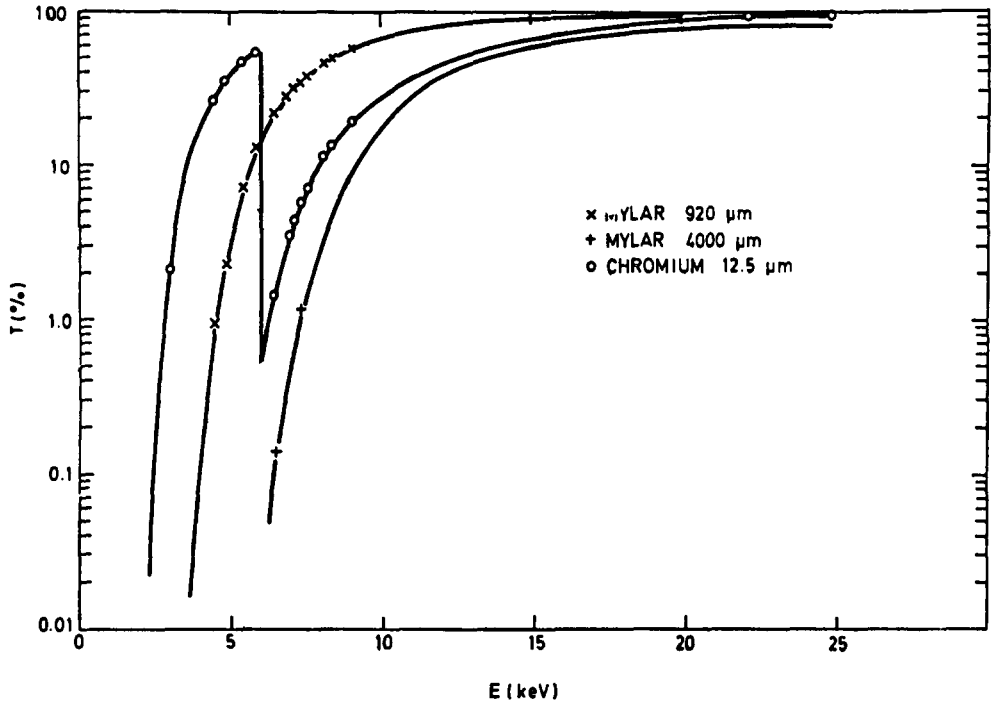

Fig. 20. X-ray transmission for three different absorbers. From ref. 101.

improving the situation is to make use of the selective absorption close to the K-edge of some suitable absorber. This problem has been investigated by Gordon and Kraner[8]), Ahlberg et al.[101]) and Ishii et al.[102]). As an illustration, we show some transmission curves by Ahlberg et al. (fig. 20). The thin mylar foil cuts out elements up to calcium and part of the electron bremsstrahlung. It is suitable for most biological and environmental samples. The thick mylar foil absorbs the entire electron bremsstrahlung background and the characteristic X-rays up to the iron group. It is useful when one wants an enhanced sensitivity for the heavier elements. The chromium absorber has a low transmission for the iron K X-rays but a fairly good transmission for lighter and heavier elements. This absorber was used with good results in the analysis of steel samples.

Hence a great deal can be done to maximize the sensitivity. Experimentally these possibilities have not been systematically exploited. In many applications a minimum detectable concentration of 10^{-6} is sufficient and it has not been deemed worthwhile to spend a considerable effort to improve on this value. However, it has been shown experimentally that one can obtain a minimum detectable concentration of 10^{-7} (corresponding to $\sim 10^{-12}$ g absolute). It is, however, necessary to realize that the sensitivities we have been discussing here refer to a pure carbon matrix. In practice, there are often some limitations due to impurities in the backing material. As discussed in section 7.8, elements such as Mn, Fe and Ni almost inevitably show up in the background spectra, thereby limiting the attainable sensitivity for these particular elements. Development work on the fabrication of ultrapure backing materials is therefore an important task.

8.2. Contamination control

When analyses are performed on absolute amounts of elements on the order of nanograms and below, it is obvious that the risk of severe contamination of the sample must be given attention. It should be recognized that these amounts are indeed very small and contaminations of the same magnitude may very easily reach the target unless great caution is taken in the sample handling procedures. Sample handling should be kept to a minimum and, when possible, samples should be collected on the substrate used during bombardement. Of course, all chemicals used for sample preparation or backing material must be sufficiently pure for the analysis in question. In our sample preparation laboratory, we avoid all use of metal tools and use

aluminium in the few cases when metals are needed. Water is, of course, both distilled and de-ionized.

The sample handling and target preparation area should be ventilated with clean air. Considering the possible effects of one dust particle of 10 μm radius and a mass of 4 ng (density assumed to be 1), it is clear that such particles in the air should be removed. This can conveniently be done by using a laboratory equipped according to clean room standards or a clean work station, which supplies a laminar flow of high quality filtered air over the work area.

The transport of samples to the accelerator is a potential opportunity for contamination and we therefore use closed containers which fit directly onto the irradiation chamber to minimize exposure of the sample to non-filtered air. Using these precautions, we are able to achieve low blank values and minimize the occurrence of spurious erratic values in the analysis.

8.3. Volatility

When the particles pass through the target, energy is deposited leading to some target heating. This could lead to the evaporation of some volatile compounds or elements. Several authors give information on this problem although no comprehensive study has been published. Valkovic et al.[90]) report from their studies of reproducibility using blood serum targets that the K and Br data indicate these elements to be evaporated in the beam. Ishii et al.[102]) find that Cl and Br are volatile at beam levels of tens of nA but that no evaporation occurs if the targets are covered with a thin layer of evaporated aluminium. Alexander et al.[103]), in their analysis of fish and sea-water samples, find Br to be volatile in sea-water samples (and not reported for fish samples). Cu levels in fish samples show some degradation with increasing beam levels, which is not the case for Ca, Zn and Fe. Campbell et al.[104]) studied biological samples and give spectra showing a dozen elements. They report that cumulative observations at 5 min intervals during bombardment at beam levels up to 1 μA show no measurable losses of the elements. In another report, Campbell et al.[86]) studied wet-digested kidney specimens but found no volatility losses during 1 h irradiation at 0.5 μA. Their results are reproduced in fig. 21. The maximum possible beam level was found to be sample dependent and wine samples were bombarded at 0.3 μA to avoid losses of Br, Pb, As and Cd. Wedberg et al.[105]) have analysed atmospheric aerosol samples for Pb and Br and find that Pb/Br ratios and the absolute amounts of these elements are reproducible even after several week's storage, indicating no evaporation of these elements. These results are supported by Cahill[47]) who found a negligible loss of Si and Br in aerosol samples and by Johansson et al.[51]) for aerosol samples. In the latter work, some compounds containing As, Se and Br and expected to be volatile were prepared but no losses were found although the results for Br were inconclusive. On the whole, evaporative losses seem to be no major problem but, for certain types of targets, some elements should be observed for their possible volatility.

It is worth mentioning that the intercalibration study discussed in the next section[106]) included analysis of real aerosol samples. These were analysed with PIXE and X-ray excited fluorescence by several laboratories. Results for all elements detected in these aerosol samples were found to be in agreement between laboratories using different methods, indicating there is no significant problem with target deterioration or volatility losses during PIXE analysis.

8.4. Accuracy and precision

The performance of PIXE under various analytical situations has been investigated by several authors. Of course, information about the accuracy and precision obtainable under different conditions is important when judging the merits of the method.

From expression (7), we expect a linear relationship between peak area and amount of an element for targets thin enough to have negligible proton and X-ray absorption. Fig. 22 shows experimental results

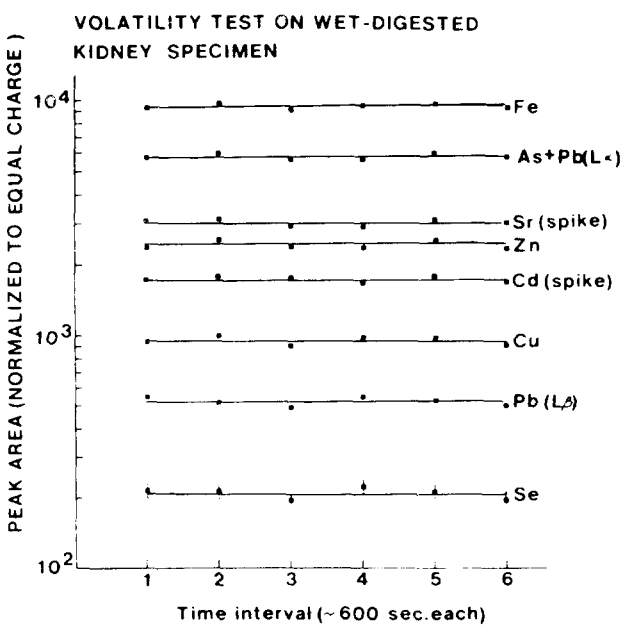

Fig. 21. Volatility test. From ref. 86.

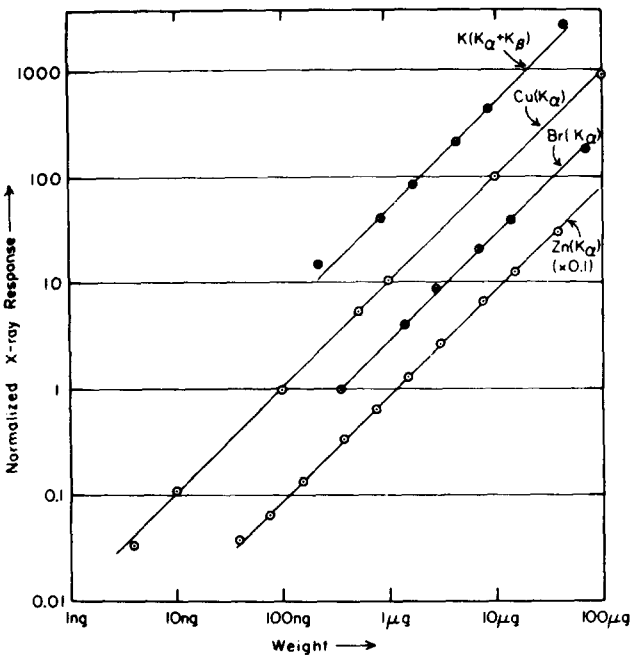

Fig. 22. Linearity test. From ref. 51.

from several targets prepared by pipetting solutions onto thin backings. After evaporation of the solvent, the targets were bombarded. The results show good agreement with the behaviour predicted.

Tests of the accuracy that can be obtained have been made by Campbell et al.[104]) who analysed Fe, Cu, Zn and Pb in animal liver with PIXE and atomic absorption spectroscopy and found overall good agreement, on the order of 10%. Bearse et al.[58]) analysed Zn in whole blood with the same methods and arrived at 10% accuracy. Johansson et al.[51]) prepared spotted targets with a Mo-containing solution and obtained 10% accuracy including target preparation uncertainties.

For Pb in samples of non-uniform kidney medulla tissue, Campbell et al.[86]) found very bad agreement between atomic absorption spectroscopy and PIXE. The same work reported PIXE analysis of NBS orchard leaves standards and showed good agreement on the average although individual fluctuations were large. The latter two examples indicate the importance of representative sampling. PIXE analysis is done on a small sample, which is an advantage in many cases, but also introduces problems in situations such as the above in which the elements studied are non-uniformly distributed on a large scale compared to the sample size. Campbell et al. correctly stress the importance of designing sampling and specimen preparation procedures based on these considerations.

During the last few years, two major interlaboratory comparisons[106,107]) have been performed and this has given excellent opportunities for checks on the accuracy of various systems. Prepared unknown samples of multielement solutions spotted on Millipore and Whatman filter papers were analysed. In the first experiment four laboratories and in the second experiment seven laboratories using PIXE participated. The results indicated PIXE accuracy of 10% or better.

Valkovic et al.[90]) have investigated the attainable precision by analysing 150 blood serum samples doped with an atomic absorption standard. For Fe, Cu and Zn they find the precision at the 1 ppm level to be 5–10%. Bearse et al.[58]) report 5–10% precision for Fe and Zn in human and mouse blood and 15–50% for Cu, Se and Rb in the same samples. Johansson et al.[51]) and Van Grieken et al.[108]) quote 3–6% for homogeneous foils and grained zircon samples and 15% for spotted Mo-solutions. Other authors report similar findings in their studies[57,66,103,104,109]). To illustrate this, fig. 23 shows some distributions of measured values obtained by Lear et al.[110]). Reported values of precision are generally worse than expected from counting statistics alone, but this problem has not been very much discussed. Probably, most cases can be explained by target preparation procedures giving non-uniform targets combined with imperfect homogeneity of the beams. Other contributions of significance may be sample deterioration during bombardment while geometry and beam integration generally are stable within statistical uncertainties. For some elements, especially for $Z \lesssim 23$, spectrum evaluation may introduce sizeable errors.

9. Comparison of different modes of excitation

9.1. α-PARTICLES

Most PIXE work has been done with protons. This has been a natural development since small proton accelerators are readily available in many laboratories. Furthermore, protons in the range 1–2 MeV have been shown to give the best sensitivity in most practical applications.

In several laboratories where α-particle beams have been available, they have been used for PIXE analysis. It is obvious that very good results can be obtained. When a high sensitivity is not essential, protons and α-particles are approximately equivalent [Cahill et al.[111])]. However, for extreme sensitivities, α-particles are of a somewhat limited value. This is especially true for energies of about 10–20 MeV, which are often used. The important factor here is the γ-ray contribu-

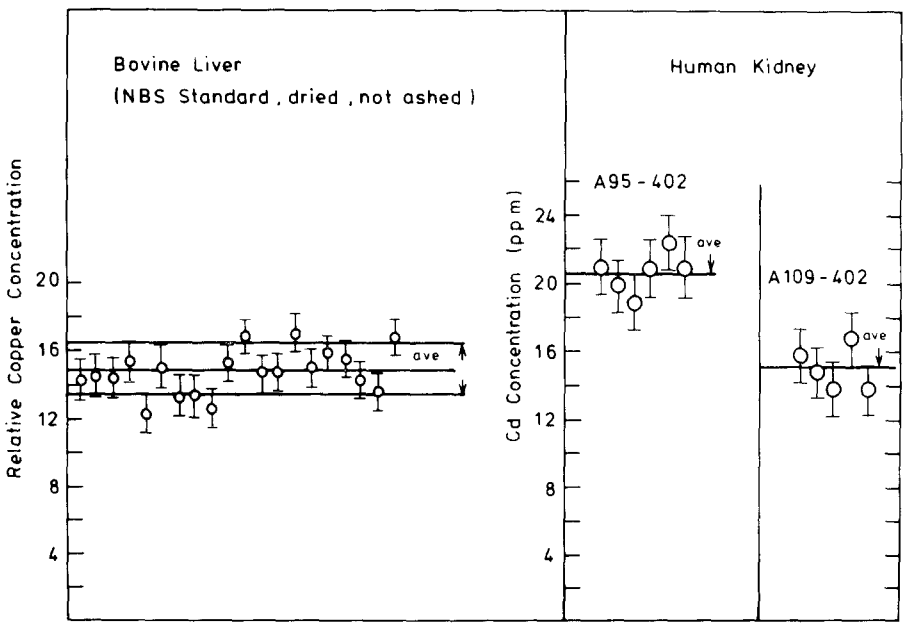

Fig. 23. Reproducibility checks. The standard deviation shown is 10%. From ref. 110.

tion to the background. Low energy α-particles (4–8 MeV) do not seem to differ much from protons with regard to sensitivity. Unfortunately, there does not exist any systematic comparison between these two modes of excitation.

There is one definite problem with α-particle excitation, namely target heating and deterioration. Due to the larger energy loss of the α-particles, it is necessary to limit the beam intensity. This offsets the advantage of a higher cross section for X-ray production.

9.2. Heavy ions

An evaluation of the merits of heavy ions in trace element analysis is rather difficult. The cross section for production of characteristic X-rays contains a Z^2 term and additional effects can increase it a factor of 10–100 above the PWBA estimate. This enhancement, however, is not a general feature but depends in a complicated way on the energy and on the particular atoms involved in the collision. Furthermore, the background is above the values obtained from a simple scaling of the proton results. The main problem at higher bombarding energies is the γ-radiation and at lower energies the continuous radiation emitted in the filling of vacancies in the molecular orbitals.

The experimental results obtained so far indicate that heavy ions do not offer any particular advantage for general trace element analysis. On the contrary, work by Gray[112]), Chemin et al.[113]) and Shabason et al.[62]) show high backgrounds and sensitivities considerably lower than for proton bombardment.

As discussed above (section 3.2), the cross section for the heavy ion production of X-rays is particularly large at low energies. Such ions have a very small penetration in matter and hence the X-radiation emitted comes from a thin surface layer. This effect is accentuated if only soft X-rays are registered by the detector. This indicates that low-energy heavy ions might be a useful analytical tool in surface physics and metallurgy. Cairns[114]) and Chemin et al.[113]) demonstrate that sufficiently high sensitivity can be attained so that fractions of a monolayer can be detected. By choosing suitable ion species and bombarding energy and by making the X-ray detection selective, this method can be made quite sensitive. This interesting development is, however, beyond the scope of the present article and will not be further discussed here.

9.3. Electrons

A convenient way of exciting X-rays is by means of electrons. They are used for analytical purposes mainly in connection with electron microscopes. The electron beam when transversing the sample excites X-rays which are recorded by means of a crystal spectrometer thereby giving information about the composition of the sample.

The X-ray cross section for electrons in the 10–100 keV range is about the same as for MeV protons. The background, which is dominated by the direct bremsstrahlung produced by the beam, is, however, much greater because of the smaller mass of the electron. This gives an increased background compared with proton excitation, between 3 and 4 orders of magnitude higher. Hence, the limit of detection is rather high, about 0.1%. An electron microprobe therefore cannot detect any trace elements but only the main constituents of a sample. Because of the thinness of the samples and the very fine focus of the beam this means, however, very small amounts on an absolute scale, about 10^{-16} g.

Another way of using electron excitation, which has found some applications, is to irradiate a sample with β-rays from a radioactive source. In combination with a silicon detector arrangement this gives a simple, yet rather powerful analytical tool. When adopted for field use, it might find some applications in, for example, geological survey work.

9.4. X-RAYS

Excitation with X-rays, the X-ray fluorescence method, is the main competitor to PIXE for energy dispersive X-ray analysis. It is therefore of great interest to make a detailed comparison between the two methods. One must, however, be very cautious in interpreting the data, since the outcome of such a comparison depends very much upon how the experimental conditions have been optimized for the two methods and also to a great extent on what kind of sample one is analysing.

An early comparison of this sort was made by Kliwer et al.[10]). Without going deeply into details, they concluded that proton excitation has a superior sensitivity.

A more detailed comparison between α- and X-ray induced analysis was made by Perry and Brady[115]). Comparing the limits of detection for 30 MeV α-particles and Mo X-rays, they found the α-particles to be slighly better for light elements ($Z<22$) and the X-rays for heavier elements. As discussed above low energy protons are considerably superior to 30 MeV α-particles. This comparison therefore indicates that PIXE, properly optimized, has a better sensitivity than X-ray fluorescence.

Cooper[116]) made a careful comparison between several different modes of excitation using both particle and photon beams. His conclusion is that the sensitivity is about the same for low energy proton and photon excitation. He then discussed the possibilities for improving the fluorescence method and claims that it has the greatest potential for further improvements. However, these conclusions do not seem to be in agreement with the spectra presented in his paper. If, for example, one takes a thick sample such as an orchard leaf, which is least favourable for PIXE, a comparison between 2 MeV proton and Mo X-ray excitation gives the following results. The ratios of the sensitivities (as defined by Cooper) are for Ca 25, Fe 4 and Pb 2. For a thin source (an aerosol sample on a mylar foil), a comparison gives the following ratios: Ca 6, Fe 50, Pb 8. A thinner sample would make the difference in sensitivity even more pronounced. Hence the spectra actually presented by Cooper demonstrate that PIXE has a superior sensitivity. The X-ray fluorescence method can, of course, be improved but it remains to be shown that this alters the overall picture. A removal of the air scattering, as suggested by Cooper, would only mean a factor of 2 in sensitivity. The use of polarized X-rays has been suggested as a means of improving the sensitivity but so far only theoretical investigations giving little hope for greater improvements have been performed.

Another comparison was made by Goulding and Jaklevic[76]) who claimed that X-ray fluorescence is superior to particle excitation. In our opinion this conclusion is based on some erroneous assumptions. In the first place, the comparison is made with 30 MeV α-particles and 4 MeV protons and not with low energy protons. As a reason for this choice, it is stated that low energy protons are of a limited value because of target heating problems and because their short range gives rise to a non-uniform irradiation. The discussion above clearly shows that these statements are incorrect. Furthermore, the sensitivity limits for particle excitation are based on theoretical calculations of the background. A comparison with experimental values or other theoretical calculations[43]) shows it to be too high by a factor of 10. The conclusions drawn in their paper are apparently affected by some computational error. What one can do using the material presented by Goulding and Jaklevic is to compare measured spectra. The X-ray fluorescence spectra shown have lower limits of detection of about 1 ppm in the most favourable case (close to the excitation energy) and 4 ppm at the iron group. This is considerably inferior to what can be achieved with PIXE (section 8.1).

Finally, Gilfrich et al.[117]) have compared sensitivities and detection limits for various X-ray methods including excitation with 5 MeV protons and α-parti-

cles. A detailed comparison is difficult since different samples were used but in general particle excitation shows by far the greatest sensitivity.

So far the discussion has been limited to the sensitivity defined as the minimum detectable concentration. It is also important to ask how the two methods compare when it comes to minimum detectable absolute amounts of matter. Then we immediately find that PIXE is by far the more sensitive method. The X-ray fluorescence method can detect absolute amounts of the order of 10^{-7}–10^{-8} g. This means that in order to realize the full sensitivity of this method the weight of the sample must be rather large, of the order of 0.1 g. With PIXE, on the other hand, amounts as small as 10^{-12} g can be detected even with a uniform beam of large cross section. By focusing the beam the lower limit of detection can be further reduced by several orders of magnitude (section 5). Hence, PIXE can be used for analysing very small samples or microscopic structures in large samples, whereas the X-ray fluorescence method is limited to those cases in which relatively large amounts of sample material are available.

This discussion hence indicates that PIXE has a greater sensitivity than the X-ray fluorescence method. The minimum detectable concentration is 10^{-5}–10^{-6} for the latter method whereas in the case of PIXE it can be pushed down to 10^{-7}. When it comes to minimum detectable amounts on an absolute scale, the superiority of PIXE is even more pronounced. For many important types of sample (air pollution, biological tissue, semiconducting material etc) this gain in sensitivity is decisive for the possibility to detect certain important trace elements. On the other hand, there are many materials for which the sensitivity offered by the fluorescence method is more than adequate. The relative simplicity of the apparatus used in this method is then a very attractive feature. Hence the two methods do not compete but complement each other.

10. Applications

10.1 Aerosol studies

An ideal situation for the application of PIXE is the investigation of many small samples, preferably as thin foils, containing 10–15 elements in amounts of 10–0.01 ng. Aerosol samples present such a case. Already in the first publication on this subject, it was indicated that PIXE can be used for aerosol studies. This was followed up and expanded to the use of cascade impactors by Willers[118]). In recent years, several extensive investigations have been reported in which full advantage of the possibilities of PIXE has been taken. For atmospheric aerosols, the natural constituents as well as the anthropogenic contributions have been studied. The aerosol at work places, especially associated with welding operations, have been subject to increasing interest as has the deposition of inhaled aerosols in the human respiratory tract.

Samples are collected on filters or by cascade impactors. As filter material both Millipore and Nuclepore have been used although Nuclepore is preferable because it is thinner and withstands more beam. Other filter materials tend to be thicker or more contaminated with elements of interest but are sometimes used when the sample is transferred to a solution for several analyses. Aerosol size fractionation is obtained by cascade impactors, where the aerosol to be sampled is drawn through jets of decreasing diameters. The aerosol is directed towards a plate covered with a thin, sticky plastic material, and particles with too high momentum to follow the streamlines of the air impinge on the plastic foil and are caught there. The samples thus collected on a filter or a thin film are directly attached to a sample holder and bombarded. This permits a minimum of sample handling. Size fractionated samples contain information on aerosol generation mechanisms and are thus of interest in atmospheric chemistry and air pollution work. Interpretation of cascade impactor data has been discussed by Johansson et al.[119]). Size distribution information is also of medical importance since deposition and removal of aerosol particles in the respiratory system is strongly size-dependent. Obviously, a large number of samples are obtained in aerosol investigations. Also, the amount of material is quite small, especially when size fractionation is employed if sampling times are to be restricted to intervals of unchanged meteorological conditions. Therefore, an analytical method with large throughput and high sensitivity must be used.

Cahill et al.[47,120]) at the Crocker Nuclear Laboratory of the University of California at Davis developed an extensive network of aerosol monitoring stations throughout California and used their fully automated PIXE system. Each station uses a two stage Lundgren impactor and an after-filter to collect the smallest particles. One week's samples then consist of seven filters and an 8″ long mylar strip which can be cut in sections down to a time resolution of 2–3 h. The samples are analysed by means of the 18 MeV α-particle beam from the Davis cyclotron. The sensitivity is on the order of a few nanograms per m^3 of air and the errors are stated to be about 10%. The capacity

is 700 samples a day and the cost per sample $5. A more detailed study of the dependence of visibility reduction on aerosol elemental composition and physical size has also been performed by the Davis group[121]). They find that, of all the parameters considered, sulphur-containing aerosols in the 0.65 to 3.6 μm size range lead to the largest effect in lowering visibility. This group has also studied the aerosol generated along a freeway in Los Angeles and find small particle lead, bromine, chlorine and sulphur in quantities depending on wind conditions and fitting reasonably well with estimates[122]). Azevedo et al.[123]) have analysed particulates near a beef cattle feed lot.

Winchester and the group of Florida State University have used PIXE for several aerosol studies. Van Grieken et al.[124]) collected parallel samples to evaluate the reliability of the sampling and analysis procedure and found good reproducibility. They added 10% quadratically to the analytical errors to account for sampling errors. Johansson et al.[125]) collected samples from a number of coastal and inland locations in North Florida. A five-stage cascade impactor was used to obtain size distributions for each element detected. A comparison of these distributions reveals typical patterns which may be used to yield information about the main aerosol sources and the generation mechanisms. As examples, the large particle elements Ti and Fe show a size-independent ratio close to that of average soils indicating soils may be their principal source, Cl is large-particle oriented and may result from bubble-bursting in the sea and the small particle elements Pb and Br originate from automotive fuel combustion.

Similar studies were undertaken in St Louis [126]) and Miami[127]). In St Louis samples were taken continuously during one week at two locations giving particle size data for 12 elements in 12 h samples of 0.7 m^3 of air each. Large variations of concentrations of some elements were related to meteorological changes during the week and indicated transport of industrial air pollution. Diurnal variations were very strong for some elements at a downtown site with the highest values being attained during nights and mornings suggesting complicated transport and mixing processes in the atmosphere. A comparison[128]) was also made with the average aerosol concentration in Florida and Bermuda samples. The results obtained indicate methods for separating the natural and antropogenic contributions to the aerosol and suggest that, in this case, some elements originate in local pollution sources.

In a study of Bermuda aerosols, Meinert [129]) found elemental concentrations and particle size distributions depending on wind speed that could be interpreted to distinguish marine and continental contributions to the aerosol. In another investigation, Johansson et al.[130]) tackled the same question using samples taken in North Florida. Examination of the data according to marine and continental air flow regimes and assuming iron to be derived predominantly from continental sources gives information about the relative importance of marine contributions to the various elements found.

Jensen and Nelson[131]) have developed a continuous timesequence total-filter sampler, designed especially for use for analysis with accelerator beams. It consists of a sliding sucking orifice, 2×5 mm^2, moving along a 0.4 μm pore size Nuclepore filter, the collected aerosol forming a streak along the filter.

Automobiles in the U.S. are now being equipped with catalytic converters for emission control. These generate sulphuric acid droplets from sulphur in the gasoline. To establish a sulphur aerosol baseline, the FSU group[132]) made a study along a freeway in Los

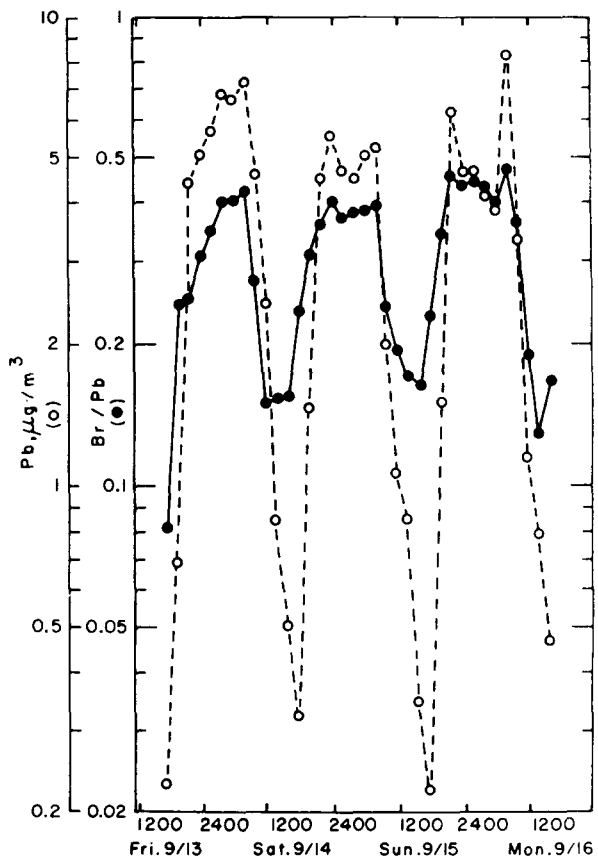

Fig. 24. Time-dependent Pb concentration and Br/Pb weight ratio relationships in a Los Angeles aerosol. From ref. 133.

Angeles before these converters became abundant, using both cascade impactors and filter streakers. The freeway was found to be a strong source of lead but not of sulphur. An illustration of the data obtained with streaker samplers in the Los Angeles study is shown in fig. 24, where Pb and Br/Pb show diurnal variations suggesting Br loss during ageing of the aerosol[133]). Wedberg et al.[105]) studied air pollution episodes in Pittsburgh collecting samples on Nuclepore filters and bombarding them with 6 MeV protons. In particular, they investigated the ratio Pb/Br in an attempt to obtain a quantitative measure of the relative industrial and automotive contribution to the total pollution. Results showed, however, that both elements are due predominantly to automobile traffic. On the other hand, pollution episodes could be characterized by studying changes of the iron and lead content of the particles.

Air pollution is, of course, not limited to the ambient air. The industrial environment has many working places where the concentration of air pollutants is very high. A systematic investigation of such places is therefore an urgent task. Since the clearance mechanism differs for various parts of the respiratory system it is important to have information about particle size distribution as well as elemental composition. Collection of the particulate matter by means of a cascade impactor followed by PIXE analysis is therefore a suitable method. The Lund group[134]) has performed an exploratory investigation of this type of air pollution in arc welding. It turned out that the aerosol concentration near the welding arc was 3–4 orders of magnitude above that in ambient air. Both the composition and particle size distribution of the aerosol depend on the welding technique and the materials being used. The size distribution data also enables a separation of welding generated aerosol components from general background in the room[135]). The results indicate that further work may contribute to minimizing the health hazards connected with welding operations.

The group at Brigham Young University[136]) measured aerosols within a copper smelter and report several carcinogenic or toxic elements including lead, arsenic, molybdenum, nickel and selenium. Using calorimetry, they also determined sulphur (IV) and sulphur (VI) and found a strong correlation between iron and sulphide, suggesting a complex of these preventing sulphide oxidation.

Much work has gone into the development of models for aerosol retention in the human respiratory tract and laboratory experiments of the deposition of specially generated aerosols. The FSU group has applied their techniques to the analysis of inhaled and exhaled ambient air to study the behaviour of real aerosols[137,138]). The results from inhalation of automotive emissions and chalk dust demostrate the feasibility of this type of study since the results generally agree with earlier work in the field. Using welding aerosols, the situation is more complicated and different results are obtained for different elements suggesting the growth of some particles during their residence in the humid bronchial atmosphere. The results from the welding study indicate the complexity of the deposition processes. Some of these results are shown in fig. 25.

10.2 Liquid samples

It is often of interest to determine the content of trace elements in solutions. The most common case is that of water solutions. The target preparation is rather straightforward. In the simplest case, one lets a drop of the aqueous solution dry on a thin carbon or plastic backing. A difficulty is that the dissolved material often crystallizes out giving a very non-uniform sample. This effect can be minimized by adding insulin to the solution. Another possibility is to use a backing such as Nuclepore filter, which is wetted by the water. Still another method to obtain a uniform sample is to use a nebulizer to spray the solution onto a backing. After repeated sprayings and evaporations of the small

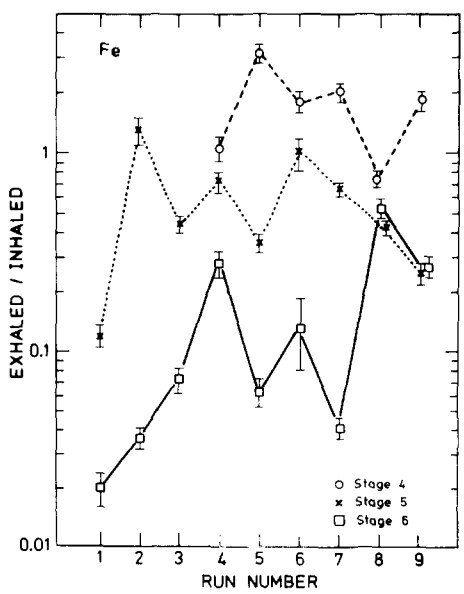

Fig. 25. Concentration ratio exhaled/inhaled for Fe in three particle size fractions. Stage 4 corresponds to aerodynamic diameters 1–0.5 μm, stage 5 to 0.5–0.25 and stage 6 to <0.25 μm. From ref. 138.

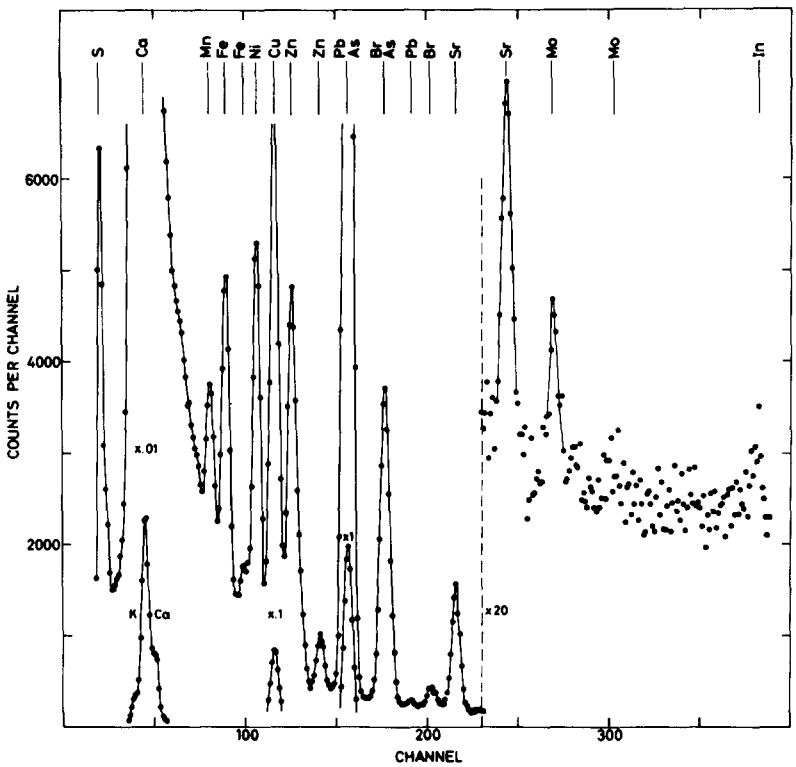

Fig. 26. PIXE spectrum of a ground water sample. From ref. 5.

droplets a uniform layer of the dissolved material is built up. An example of such an analysis is shown in fig. 26, which exhibits a spectrum recorded with a sample of ground water from North Sweden. It is obvious that this is a rapid, sensitive and accurate way of analysing water. A special feature of this particular spectrum is the high concentration of arsenic. The reason for this is that the sample was taken close to a mine containing gold ore with a high arsenic content. This indicates that it might be possible to use the trace element concentration in ground water as an indicator in ore prospecting.

The sensitivity can be increased by preconcentration of the water solution. However, one might run into difficulties because of the presence of considerable amounts of light elements in the solution. For example, ground water contains calcium salts and sea water sodium chloride. Targets prepared by preconcentration of such water samples will be rather thick which tends to decrease sensitivity and accuracy. One possible solution to this problem is the procedure used by Van Rinsvelt et al.[139]). They prepared thick targets by freeze-drying water samples. The residue was pressed into a pellet. The accuracy was improved by the use of internal standards. An interesting method of preconcentrating the metal trace elements in water solutions has been investigated by Lochmüller et al.[140]). They used membranes inpregnated with a cation exchange resin. When placed in a water solution these membranes absorb the metal ions. After rinsing and drying the membranes were irradiated with 3 MeV protons. Concentrations as small as 10^{-8} molar lead in aqueous solutions have been measured. Quantitative analysis naturally requires a calibration of the ion uptake in the membrane.

The case of body fluids such as blood, serum, urine etc is discussed in connection with other biological samples in the next section.

The content of trace elements in oil is sometimes of great interest. It is known that crude oils from different oilfields have varying trace element content. The trace elements therefore constitute a kind of "fingerprint" of the oil and can be used for identification purposes, for example in connection with oil pollution. Johansson et al.[5]) showed that by heating an oil drop on a carbon backing and analysing the sample by PIXE a rapid and accurate determination of all the major trace elements could be obtained.

10.3 Biological and medical samples

It is well-known that the quantitative determination of trace element concentration in biological tissue is an important problem. It has also some medical implications. Several diseases are known to be associated with the deficiency or overabundance of various trace elements. There are also the problems of the toxic effects of pollutants from modern industry. Well-known examples are cadmium, mercury and lead poisoning.

Many of the important trace elements are present in concentrations of 1 ppm or higher. It is therefore possible to use PIXE for a rapid, multielemental determination. This possibility has been explored by a great number of research workers. The cases investigated include practically all major animal and human organs as well as various other biological materials. The results obtained demonstrate in a very convincing way that PIXE is a powerful method for trace element determinations in samples of this type. A typical spectrum is depicted in fig. 27.

The target preparation technique is important in this connection. The biological material must be brought into a form which is convenient for irradiation but without any loss of trace elements or introduction of contaminations. Jundt et al.[56]) compared three different techniques:

1) Fresh tissue samples were deep-frozen, then cut with a microtome. Small sections were deposited on thin formvar backings.
2) Fresh tissue samples, formalin-fixed and paraffin-embedded, were sectioned, deposited on a thin backing and then deparaffinized.
3) Fresh tissue samples were mixed with an equal amount of distilled, de-ionized water and then homogeneized in a high speed blender.

The first-mentioned method turned out to be the best one. The deep-frozen sections are easy to handle and adhere well to the backing. In the other two methods a certain loss of some elements was found.

Kliwer et al.[10]) used vacuum freeze drying to reduce the sample to a powder which then was fixed to the backing by means of a very dilute polystyrene glue. They also used ashing at 500 °C. Since the organic material burns off, the background is reduced which improves the sensitivity. A draw back of this method is that volatile elements might be lost.

Walter et al.[52,141]) mounted tissue sections on a thin plastic backing. Various backing materials were investigated and Nuclepore was found to be the best one. Granular samples such as lyophilized tissue were sandwiched between two layers of thin plastic film.

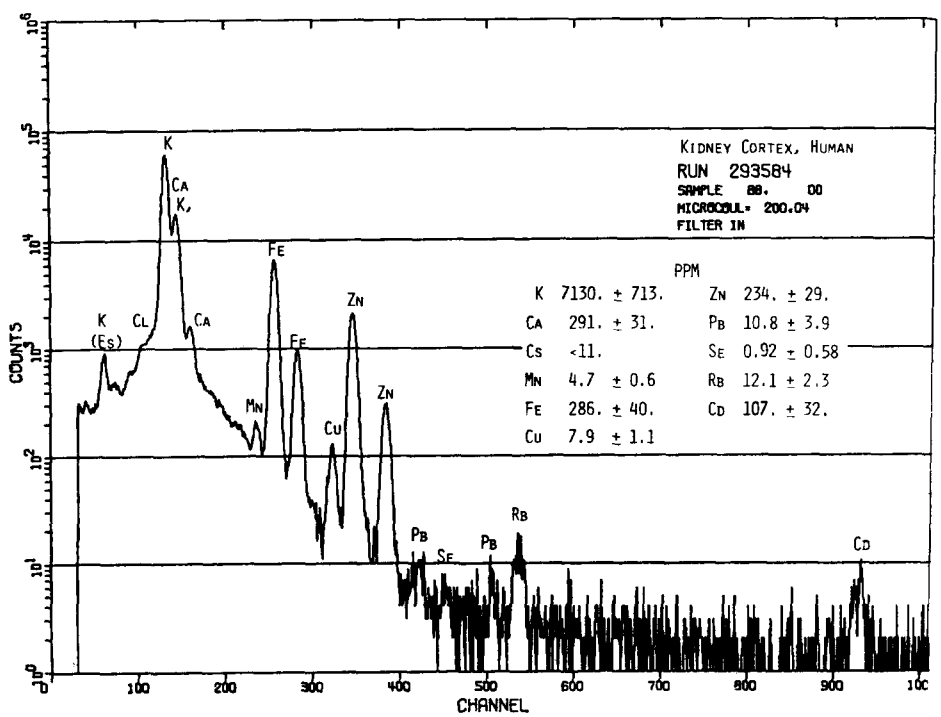

Fig. 27. Spectrum from PIXE analysis of human kidney cortex. From ref. 142.

These papers contain a great number of spectra illustrating the analysis of various biological samples.

Campbell et al.[86]) use wet digestion, which they find very satisfactory. 0.25 g of the sample is dissolved in ultrapure nitric acid. A drop of the acidic solution is evaporated to dryness on a thin carbon foil. These workers discuss the target preparation technique in great detail and they also present a very illuminating discussion of other aspects of the PIXE technique, such as standardization, reproducibility and accuracy.

Mangelson et al.[142]) report some difficulties with the wet digestion technique and use instead low temperature dry ashing. The ash remaining from the organic sample is dissolved in nitric acid and small aliquots of the resulting solution are deposited on a Nuclepore filter.

Lear et al.[107]) use powdered samples (high temperature ashing or freeze-drying) placed on a formvar film. The powder is covered by a second formvar film. They eliminate the weighing or doping of the sample by recording the elastically scattered protons from the sample. Linearity tests show that the intensity of the scattered protons is a good measure of the amount of target material exposed to the beam.

Van Rinsvelt et al.[139]) studied the use of thick targets of biological material. The samples were freeze-dried, a suitable doping added and the material pressed into a pellet.

Most of the work performed so far has been feasibility tests but some investigations of specific biological problems have been reported. Umbarger and Malanify[143]) used PIXE to distinguish between laboratory grown sterilized screw-worm flies and natural screw-worm flies captured in the field. Van Rinsvelt et al.[144]) studied the trace element content in various insects. Holst[145]) investigated the changes of the chlorine concentration in embryos of quasil eggs when the eggs were treated with 2,4–D and 2,4,5–T. Algae living in arctic snow and in Icelandic geysers were studied by Fjerdingstad et al.[146]). The effect of varying salinity on elemental relationships in bean leaves has been investigated by Murray et al.[147]). Stanford et al.[148]) studied the relationship between the amount of metal in the soil and the metal uptake in the plant Plantago lanceolata.

A special case is the investigation of body fluids, i.e. blood, serum, saliva, etc. Samples are usually prepared by allowing a drop of the fluid to dry on a thin carbon or plastic backing. In some cases problems arise because of flaking or when the backing is torn by the deposit. A solution to these problems might be to cover the sample by a thin plastic foil. It is also possible to prepare very thin samples from such fluids by drying and ashing. Bearse et al.[58]) discuss in detail such a procedure for human whole blood. They investigated also the precision, accuracy and linearity of the method.

Some large molecules of biological interest, e.g. enzymes, contain small amounts of metal, essential for their chemical activity. A well-known example is hemoglobin, which contains 0.3% iron by weight. For analysis of such substances PIXE should be an ideal method. Since usually only small amounts are available, high sensitivity is needed. By measuring the metal content in a sample, one can both determine the amount of protein present and check its purity. Such measurements have been reported by Young et al.[13]) and Walter et al.[141]).

Most investigations of medical samples performed so far have mainly been of an exploratory nature. However, some results of medical interest, illustrating the usefulness of the method, have been reported. Kliwer et al.[10]) investigated patients who had been undergoing hemo-dialysis. Skin samples of the patients showed abnormal amounts of tin, cadmium and molybdenum and a deficiency of bromine. Watson et al.[42]), also investigating such patients, found the same bromine deficiency and an excess of zinc in blood serum samples. Another investigation of blood serum after hemodialysis by Lear et al.[107]) showed the same deficiency of bromine, a strong increase of iron but a decrease in zinc. The trace element content of

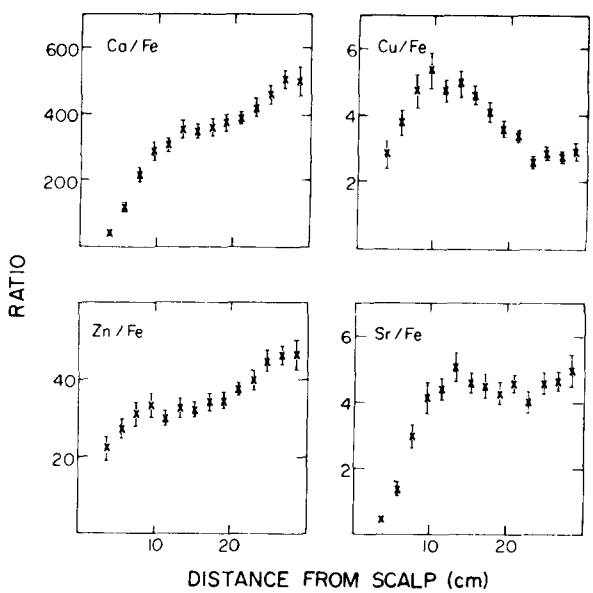

Fig. 28. Variation of the relative concentration of trace elements along human hair as a function of distance from the scalp. From ref. 90.

malaria infected blood in mice was studied by Barnes et al.[49]). In the red cells, an increase of K, Ca, Cu and Zn was found while the plasma showed an increase for Ca and a decrease for K, Cu and Fe. Campbell et al.[104]) studied the toxic effects of lead and zinc in growing foals, especially the interaction between the toxic effects of these two elements. Mangelson et al.[142]) making an extensive study of the trace element content in autopsy tissue found a correlation of some concentration patterns with incidence of diabetes mellitus. Lear et al.[107]) investigated the cadmium concentration in kidney and found a correlation with age and disease state. Investigations of trace element concentrations in hair have been performed by Jolly et al.[149]), Valković et al.[150]) and Horowitz and Grodzins[70]). The trace element distribution along the hair gives information about the previous elemental concentration in the body as well as previous environmental effects. An example of such measurements is shown in fig. 28.

Hence the study of trace element variations in biological and medical samples presents many ideal and important application for PIXE analysis.

10.4 Thick samples

Sometimes thick samples are used for PIXE analysis. The main reason for using a thick sample as target is its simplicity. No complicated target preparation is needed. The sample, for example a thick tissue section, is just mounted in a holder and irradiated directly. An advantage is that the risk of introducing contaminants is minimized. In some cases the preparation of thin samples is difficult or impossible. Examples are biological tissues such as bone or teeth, metallurgical samples and various solid state materials. In the cases where one is interested in the microstructure of the sample, for example in the depth distribution of impurities, any target preparation is, of course, excluded.

There are, nevertheless, several disadvantages connected with the use of thick samples. A major problem is that of the non-uniformity of most samples. Even in a thick sample most of the X-rays originate in a thin surface target as illustrated in fig. 29. This is especially true for low particle energies and for low energy X-rays (light elements). Therefore the results obtained might not reflect the composition of the bulk of the sample. A further difficulty is heat generation in the sample. The whole energy content of the particle beam is deposited in the sample. Excessive deterioration will therefore occur unless one uses quite low beam currents, resulting in low sensitivity.

Calculation of the elemental composition from the X-ray yield is considerably more difficult for a thick sample than for a thin one. Since the energy of the

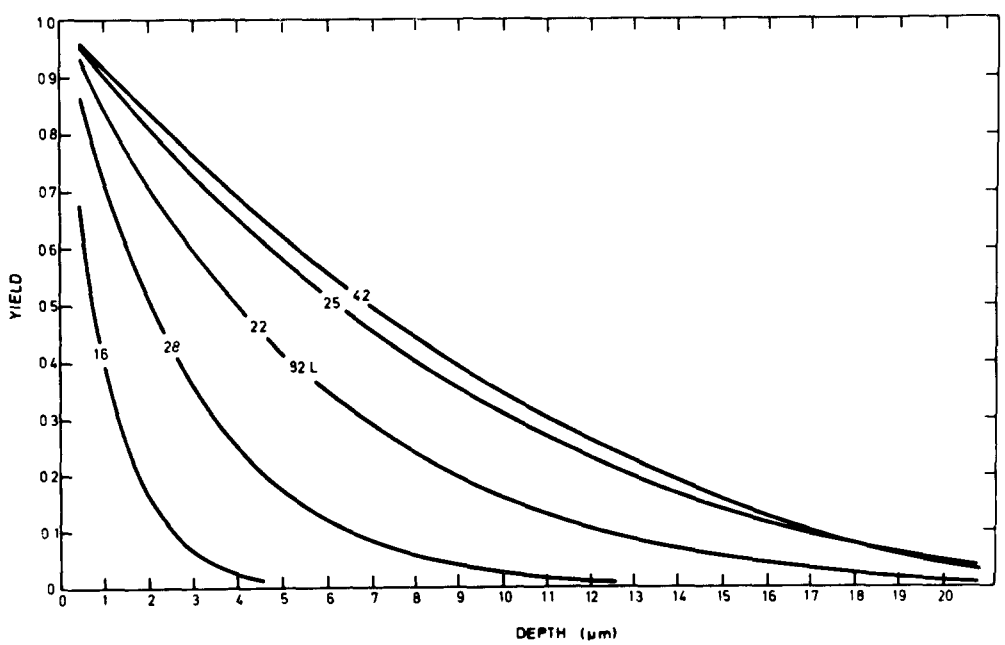

Fig. 29. X-ray yield as a function of depth in a steel sample. The curves correspond to the indicated Z-values. The sample was bombarded with 2.5 MeV protons. From ref. 101.

incident particles decreases while they transverse the sample, it is necessary to integrate the X-ray production over the entire particle path. This requires in principle knowledge of the composition of the matrix as well as of the distribution of the trace elements. In the case of uniform samples, it is possible in practice to perform such a calculation. The experience in our laboratory is that an absolute determination can also be achieved for thick targets. The accuracy is not considerably worse than for thin samples.

One possibility to circumvent the difficulties connected with an absolute determination of the composition of a thick sample is to use an internal standard (section 6).

Several examples of thick sample analysis can be found in the literature. In most cases it is biological material such as leaf, animal tissue etc which has been analysed. These examples demonstrate that thick samples are convenient for a rapid survey of the trace element content.

A quantitative analysis has been attempted in some cases. Shabason et al.[62]) used heavy ions for analysis of thick targets. They calculated efficiency curves which can be used for determination of the trace element concentration in various matrices. As examples they show spectra for a beryllium sample, household aluminium foil, and ashed coal.

Analysis of thick steel samples is discussed by Ahlberg et al.[101]). The main problem in this case is the very strong X-ray emission from the iron matrix, which tends to mask the small trace element peaks in the spectrum. A careful selection of X-ray absorbers is therefore essential. Even under these rather unfavourable conditions concentrations as low as 40 ppm could be measured.

Another example of the use of thick samples is an investigation by Ahlberg and Akselsson[154]) of the trace elements in human teeth. Detection limits of the order of 1–10 ppm were obtained. The accuracy and precision of the method were studied in detail and special attention was paid to some complicating effects such as the enhanced yield due to the secondary production of X-rays and the influence of the surface roughness. The enhancement effect is in general quite small but in this special case it amounted to 15% for potassium.

The effect of the surface roughness is a general problem in the measurement of thick targets. The absorption of the X-rays in a target depends on its orientation (section 7.9). A rough surface corresponds to an orientation which varies over the surface of the target. The net effect of this variation is an increase of the absorption relative to that of a perfectly flat surface by an amount depending on the height differences of the target surface. In the investigation mentioned above, height differences of 9 mg/cm^2 were estimated to give a 30% decrease of the X-ray yield for the lightest elements (between Si and Ca).

Direct measurement of the trace element content in various solid state materials is another application of PIXE. Young et al. report an investigation of a thick Si wafer[13]). Larsson[155]) detected small amounts of copper in a silicon crystal. Gray et al.[111]) have studied various semiconductor systems and Demortier[156]) the analysis of palladium in a copper matrix. Strashinskii et al. [157]) investigated a thick beryllium sample. The diffusion of Lanthanum on the surface of a NaCl crystal was studied by Saltmarsh et al.[12]). A combination of the channeling effect and PIXE was applied by Chemin et al.[113]) for an investigation of phosphorus and sulphur implants in germanium crystals.

The PIXE method has certain possibilities for obtaining information about the variation in concentration in a thick sample. This clearly has great practical implications, for example, in determining the depth profiles in materials which have been doped by ion implantation. The X-ray yield depends on the experimental parameters and on the distribution of the element to be measured. Variation of the experimental parameters should then make it in principle possible to extract information about the distributions. Various possibilities have been studied. Reuter et al.[158]) investigated the effect of varying the beam energy, Feldman et al.[159]) and Pabst[160]) the effect of variation in the target orientation relative to the beam and the detector. Unfortunately the X-ray yield is rather insensitive to the details of the trace element distribution but, in some simple cases, useful information can be obtained.

A different approach to this problem was taken by Ahlberg[161]). He utilizes the fact that the K_α and K_β X-rays from a certain element are absorbed to a different degree in the sample due to their slightly different energies. Hence the α/β ratio depends on the path length of the X-rays in the sample. X-rays emitted from the interior of the sample have a smaller α/β ratio than those from the surface. Ahlberg demonstrates that it is indeed possible to determine both the surface and bulk concentration in one single run.

10.5 Miscellaneous applications

There have been reported several applications in other fields of science than the ones discussed above.

They will be briefly described here in order to show the versatility of PIXE analysis.

A geological application is reported by Van Grieken et al.[109]). Using very small samples (<mg) they measured the zirconium-hafnium ratio in zircons. Clark et al.[46]) analysed several USGS standard rocks and demonstrated the possibility of measuring up to 28 elements by combining X-ray and γ-ray detection.

In the forensic sciences an application is reported by Barnes et al.[14]) who studied the residues from gun firing.

An archeological sample (shard pigment) was analysed by Gordon and Kraner[8]). Chromium and manganese were detected in the presence of large amounts of iron by means of the critical absorber technique. Ahlberg et al.[162]) studied touch-stones from the bronze age and found traces of gold on the surface of the stones, indicating that they have been used for estimating the quality of coins or other objects of gold.

Investigation of solid state materials has been discussed in connection with thick samples. However, one can sometimes use thin samples in this connection. Thomas et al.[91]) studied thin films of semiconducting chalcogenide glasses as well as the purity of thin boron films. Pabst and Schmid[163]) determined the zinc concentration in an epitaxial layer of InSb. Poncet and Engelmann[164]) studied the linearity and sensitivity in measurements on thin metal foils.

Martin et al.[165]) have used PIXE for a determination of bromine and zinc levels in wheat flour.

10.6 Chemical state analysis

A characteristic X-ray is emitted from an atom with a vacancy in, e.g., the K-shell. If other vacancies in the electron shells are present during this process, the binding energies shift slightly and therefore the energy of the emitted X-ray also shifts somewhat. Richard et al.[166]) report proton and helium bombardment of Ti using high resolution crystal spectrometers and find satellite lines resulting from additional electron vacancies tens of eV from the original position. Burkhalter et al.[167]) have investigated the energy shifts of regular as well as satellite lines for chemical states of Al and report detectable changes as large as a few eV for some lines. Other X-ray studies of chemical states have also been reported by Deconninck[168]) using charged particles and by Hurley and White[169]) and Gohsi et al.[170]) using X-ray excitation.

11. Use of nuclear reactions in combination with X-ray emission

As discussed previously, one of the problems with PIXE is that the lightest elements cannot be detected with the use of standard silicon detectors. One solution to this difficulty is to use special detectors, e.g. windowless silicon detectors or specially designed proportional counters. Another possibility is to make use of the nuclear reactions induced in the target. These reactions are an important part of the background (section 4.1) and set a limit to the sensitivity attainable for heavier elements. They are however, also characteristic for the nuclides being present in the bombarded sample and can therefore be used for analytical purposes. Since the same target and the same beam as in the X-ray emission studies can be used, a short discussion of this subject is warranted.

The reactions of interest here are elastic and inelastic scattering of protons, (p, p') and (p, p'γ), and capture of protons, (p, γ). For some nuclides capture of protons with particle emission, e.g. (p, $\alpha\gamma$) has also been used. For α-particles the main reaction of interest is elastic scattering, (α, α'). These reactions can be applied in two ways, by detecting either the emitted γ-radiation or the scattered particles. In the former case, the silicon detector used for X-ray measurements is replaced by a large germanium detector. In the latter case, a solid-state particle detector is built into the irradiation chamber so that particles scattered backwards are registered.

An important fact to note in connection with these reactions is the resonant character of the cross-section curve. This is especially true for lower proton energies and for the capture reactions. The combination of resonance excitation and characteristic γ-ray spectra makes this method very selective. In analysing a thin target the proper choice of bombardment energy gives an enhanced sensitivity for a certain element. Thus the method is not multielemental but since only a rather limited number of elements are of interest in this connection this is no serious drawback. In the case of a thick target, the proton energy decreases and several resonances in various nuclides can be excited. One then must rely upon the possibility of being able to resolve the γ-ray spectrum into its components.

It should be pointed out that in the case of resonant nuclear reactions the amount of material actually sampled is determined by the width of the resonances and is in general much smaller than the weight of the whole sample. This fact makes the calculation of the concentrations somewhat complicated requiring de-

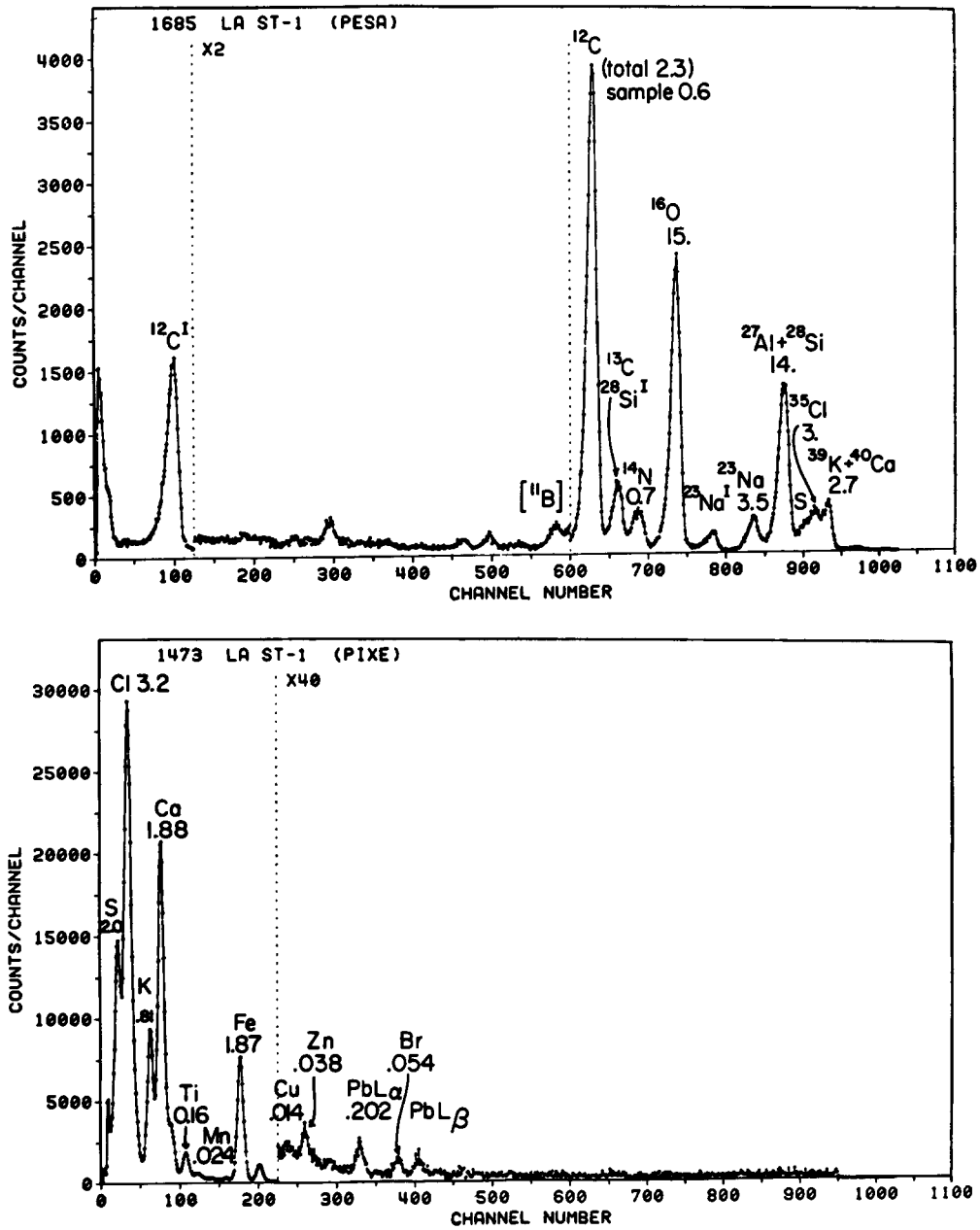

Fig. 30. Proton scattering spectrum and PIXE spectrum for the same air particulate sample. From ref. 174.

tailed knowledge of the cross-section curve. Furthermore, the homogeneity of the sample is very important.

In recent years there has been a considerable interest in using nuclear reactions for analytical purposes but the limited space does not permit any detailed account. A review of this subject can be found in ref. 171. Only the attempts to combine PIXE with nuclear reactions will be shortly mentioned.

Clark et al.[46]) discuss this technique in considerable detail and apply it to the analysis of geological samples. By irradiating a sample with 4 MeV protons and combining X-ray and γ-ray detection they were able to determine 28 elements from Li to Ba with good accuracy. The combination of PIXE with elastic scattering has been applied by Cahill et al.[172]) (α-particles) and Nelson et al.[173,174]) (protons) to air pollution studies. Very beautiful spectra containing well defined peaks for all the light elements from B to Cl are obtained.

One such spectrum is shown in fig. 30. A drawback of the scattering method with particle detection is that fairly high particle energies ($\sim$15 MeV) are needed in order to resolve adjacent elements.

12. Costs

It is sometimes claimed that PIXE, since it requires access to a proton or heavy ion beam, is expensive and difficult to apply routinely. It is therefore of considerable interest to discuss these aspects of the method.

First of all it is important to realize that there exists today a large number of small accelerators suitable for PIXE analysis. Many of these are no longer of interest for nuclear physics research and it is therefore of potential interest to find alternative applications. Hence it is not surprising to find that several accelerators today are used for PIXE analysis, partly or full time. To take a few examples, the Davis cyclotron operates on a commercial basis analysing air pollution samples with a capacity of 700 per day. The 4 MeV Van de Graaff accelerator at the Bohr institute in Copenhagen has in recent years been used exclusively for PIXE analysis. At the Lund Institute of Technology half the available beam-time of a 4 MeV Van de Graaff generator has since 1968 been used for development work on PIXE.

When a project is run commercially it is easy to estimate the costs. At Davis the cost per sample is less than \$5. We estimate that at Lund the cost for a 10 min analysis is \$10. It is important to realize that most of the costs goes into labour for preparing and handling samples. The capital cost of the accelerator is usually quite small if an older accelerator is used. But even paying the full capital costs of a new accelerator does not increase the cost per sample considerably. A small electrostatic accelerator in the 2 MeV range costs about \$200 000. If it is amortized over a period of ten years, the capital cost per year is about \$30 000. An accelerator used full time can analyse on the order of 100 000 samples a year. Hence the capital cost of the accelerator per sample is about \$.0.3 This is completely negligible compared to the labour costs, even if one takes into account that an accelerator will need more maintenance and a larger experimental area than the equipment used in other types of analysis. The conclusion must be that the need to have access to a particle beam by no means makes PIXE an expensive method. An interesting conclusion is that from an economical point of view it would be a good investment to buy a new accelerator for use in PIXE analysis. It may be mentioned that the recent purchase of a new 3 MV tandem accelerator by the Lund Institute of Technology was motivated largely by its usefulness in PIXE analysis.

In this connection it is interesting to discuss the lower limit to the bombarding energy. If energies substantially lower than 1 MeV can give satisfactory sensitivity, there might be a possibility of using small, cheap accelerators, such as cascade generators, for PIXE analysis. The discussion in section 5 indicates that the sensitivity decreases with decreasing bombarding energy in the region below 1 MeV. Practical experience is rather limited. Beezhold[175]) used 285 keV protons for a study of contamination in SiGe samples. Bales et al.[66]) found it possible to use protons with an energy as low as 100 keV, although the sensitivity was considerably lower than at higher energies. Hence, it does seem possible to use quite small accelerators for at least certain types of PIXE analysis, making it even less expensive.

It is also of interest to compare the values quoted above with the cost for other types of analysis. The cost for neutron activation, which still is used extensively for the analysis of biological and environmental samples, is approximately ten times higher than for PIXE. In comparison with other methods such as atomic absorption or emission spectroscopy, one also finds that PIXE is economically competitive.

13. Conclusions

It is obvious from the account presented here, that PIXE has in a very short time been developed into a powerful analytical tool. The increasing number of practical applications demonstrate its usefulness and the results of this development work indicate that it is competitive with the standard methods. It might be instructive to end this paper by summarizing the salient features of the method, both advantageous and disadvantageous.

Advantages

1) PIXE is multielemental. Up to 20 elements can be determined simultaneously.
2) Practically the whole periodic table can be covered in one single run and the sensitivity is fairly constant over this region. For elements with $Z>12$, it does not deviate more than a factor of 3 from the mean value.
3) The sensitivity is very high. In terms of minimum detectable concentration it is 10^{-6}–10^{-7}. Since very small samples can be analysed, this means minimum detectable amounts as low as 10^{-15} g.

4) PIXE is fast. For most samples a running time of 2–5 min is sufficient. If the resulting spectra are fed into a computer they can be analysed and a print-out be available a few minutes after a run.
5) Very small samples can be analysed with full sensitivity. Using the microprobe technique, even microstructures can be analysed.
6) PIXE is non-destructive.
7) Good economy. Taking into account the fact that information for all elements above a certain, quite low, concentration are obtained in a single run of short duration, it is cheaper than most other methods.

Disadvantages:

1) There occur interferences between K and L X-rays from light and heavy elements, respectively, and between K_α and K_β peaks in neighbouring elements. This has a negative effect on the sensitivity. Increased detector resolution could give great improvements. Another possibility is to analyse the X-rays by means of a crystal spectrometer. Then, however, the multielemental character of the method is lost.
2) PIXE is best suited for thin samples (thickness less than 1 mg/cm^2). Thick samples can also be used but the analysis of the resulting spectra is more complicated and the accuracy is reduced. One possibility to improve this situation is to use internal standards.

The advantages seem to be considerably greater than the disadvantages. Hopefully, PIXE will be further improved and established as a standard analytical method.

Note added in proof: Goulding has very recently (PIXE Conference, Lund, Sweden, August 1976, to be published in Nucl. Instr. and Meth.) revised the calculations reported in ref. 76. His new results concerning the sensitivity of the PIXE method are in good agreement with the figures presented in the present paper.

References

[1]) T. B. Johansson, R. Akselsson and S. A. E. Johansson, Nucl. Instr. and Meth. **84** (1970) 141.
[2]) R. L. Watson, J. R. Sjurseth and R. W. Howard, Nucl. Instr. and Meth. **93** (1971) 69.
[3]) R. G. Flocchini, P. J. Feeney, R. J. Sommerville and T. A. Cahill, Nucl. Instr. and Meth. **100** (1972) 397.
[4]) J. L. Duggan, W. L. Beck, L. Albrecht, L. Munz and J. D. Spaulding, Advan. X-ray Anal. **15** (1972) 407.
[5]) T. B. Johansson, R. Akselsson and S. A. E. Johansson, Advan. X-ray Anal. **15** (1972) 373.
[6]) G. Deconninck, J. Radioanal. Chem. **12** (1972) 157.
[7]) J. W. Verba, J. W. Sunier, B. T. Wright, I. Slaus, A. B. Holman and J. G. Kulleck, J. Radioanal. Chem. **12** (1972) 171.
[8]) B. M. Gordon and H. W. Kraner, J. Radioanal. Chem. **12** (1972) 181.
[9]) G. Demortier, J. Lefebre and C. Gillet, J. Radioanal. Chem. **12** (1972) 277.
[10]) J. K. Kliwer, J. J. Kraushaar, R. A. Ristinen, H. Rudolph and W. R. Smythe, Bull. Am. Phys. Soc. **17** (1972) 504.
[11]) A. Pape, J. C. Sens, P. Fintz, A. Gallmann, H. E. Gove, G. Guillaume and D. M. Stupin, Nucl. Instr. and Meth. **105** (1972) 161 and Report CRN-LPNIN 7202, Centre de Recherches Nucléaires et Université Louis Pasteur, Strasbourg, France.
[12]) M. J. Saltmarsh, A. van der Woude and C. A. Ludemann, Appl. Phys. Lett. **21** (1972) 64.
[13]) C. J. Umbarger, R. C. Bearse, D. A. Close and J. J. Malanify, Advan. X-ray Anal. **16** (1973) 102.
[14]) F. C. Young, M. L. Roush and P. G. Berman, Int. J. Appl. Rad. Isotop. **24** (1973) 153.
[15]) B. K. Barnes, L. E. Beghian, G. H. R. Kegel, S. C. Mathur and P. Quinn, J. Radioanal. Chem. **15** (1973) 13.
[16]) F. Folkmann, J. Phys. E. **8** (1975) 429.
[17]) I. R. Lukas, Report (1973) CRD-55-1973, Bucharest, Romania.
[18]) V. Valković, Contemp. Phys. **14** (1973) 415.
[19]) J. D. Garcia, R. J. Fortner and T. M. Kavanagh, Rev. Mod., Phys. **45** (1973) 111.
[20]) E. Mezbacher and H. W. Lewis, *Handbuch der Physik*, vol. 34 (Ed. S. Flügge; Springer Verlag, Berlin, 1958) p. 166.
[21]) G. Basbas, W. Brandt and R. Laubert, Phys. Rev. **A7** (1973) 983.
[22]) J. Bang and J. M. Hansteen, Kgl. Dan. Vid. Selsk. Mat. Fys. Medd. **31** (1959) no. 13.
[23]) J. M. Hansteen and O. P. Mosebekk, Nucl. Phys. **A201** (1973) 541.
[24]) J. D. Garcia, Phys. Rev. **A1** (1970) 280.
[25]) J. S. Hansen, Phys. Rev. **A8** (1973) 822.
[26]) J. M. Hansteen, Sci./Techn. Report no. 79, University of Bergen, Bergen, Norway.
[27]) C. H. Rutledge and R. L. Watson, At. Data and Nucl. Data Tables **12** (1973) 195.
[28]) G. S. Khandelwal, B. H. Choi and E. Merzbacher, At. Data **1** (1969) 103; B. H. Choi, E. Merzbacher and G. S. Khandelwal, At. Data **5** (1973) 291.
[29]) W. Brandt, R. Laubert and I. Sellin, Phys. Rev. **151** (1966) 56.
[30]) P. Richard, T. I. Bonner, T. Furuta and I. L. Morgan, Phys. Rev. **A1** (1970) 1044.
[31]) G. A. Bissinger, J. M. Joyce, E. J. Ludwig, W. S. McEver and S. M. Shafroth, Phys. Rev. **A1** (1970) 841; G. A. Bissinger, S. M. Shafroth and A. W. Waltner, Phys. Rev. **A5** (1972) 2046; S. M. Shafroth, G. A. Bissinger and A. W. Waltner, Phys. Rev. **A7** (1973) 566; C. E. Busch, A. B. Baskin, P. H. Nettles, S. M. Shafroth and A. W. Waltner, Phys. Rev. **A7** (1973) 1601.
[32]) A. Fahlenius and P. Janho, Ann. Acad. Sci. Fennicae Series A, VI Physica **367** (1971) 1.
[33]) R. C. Bearse, D. A. Close, J. J. Malanify and C. J. Umbarger, Phys. Rev. **A7** (1973) 1269.
[34]) L. M. Winters, J. R. Macdonald, M. D. Brown, L. D. Ellsworth and T. Chiao, Phys. Rev. **A7** (1973) 1276.

[35]) R. B. Liebert, T. Zabel, D. Miljanić, H. Larson, V. Valković and G. C. Phillips, Phys. Rev. **A8** (1973) 2336; R. P. Chaturvedi, R. M. Wheeler, R. B. Liebert, D. J. Miljanić, T. Zabel and G. C. Phillips, Phys. Rev. **A12** (1975) 52.

[36]) R. Lear and T. J. Gray, Phys. Rev. **A8** (1973) 2469; T. L. Criswell and T. J. Gray, Phys. Rev. **A10** (1974) 1145.

[37]) R. Akselsson and T. B. Johansson, Z. Physik **266** (1974) 245.

[38]) W. Bambynek, B. Craseman, R. W. Fink, H. U. Freund, H. Mark, C. D. Swift, R. E. Price and P. V. Rao, Rev. Mod. Phys. **44** (1972) 716.

[39]) H. U. Freund, X-ray Spectrom. **4** (1975) 90.

[40]) J. H. Scofield, Phys. Rev. **A9** (1974) 1041.

[41]) S. I. Salem and C. W. Schultz, At. Data **3** (1971) 215.

[42]) R. L. Watson, C. J. McNeal and F. E. Jenson, Advan. X-ray Anal. **18** (1975) 288.

[43]) F. Folkmann, C. Gaarde, T. Huus and K. Kemp, Nucl. Instr. and Meth. **116** (1974) 487.

[44]) F. Folkmann, J. Borggren and A. Kjeldgaard, Nucl. Instr. and Meth. **119** (1974) 117.

[45]) R. G. Musket, Nucl. Instr. and Meth. **117** (1974) 385.

[46]) P. J. Clark, G. F. Neal and R. O. Allen, Anal. Chem. **47** (1975) 650.

[47]) T. A. Cahill, University of California at Davis, Report (1973) UCD-CNL-162; F. P. Brady and T. A. Cahill, Report (1973) UCD-CNL-166.

[48]) J. F. Harrison and R. A. Eldred, Advan. X-ray Anal. **17** (1974) 560.

[49]) B. K. Barnes, R. M. Coleman, G. H. R. Kegel, P. W. Quinn and N. J. Rencricca. Advan. X-ray Anal. **18** (1975) 343; B. K. Barnes, L. E. Beghian, G. H. R. Kegel, S. C. Mathur, A. Mitler and P. W. Quinn, Proc. 3rd Conf. on *Application of small accelerators*, vol. 1, CONF 741040-P1 (1974) p. 327.

[50]) K. Kemp, F. Palmgren Jensen, J. Tscherning Møller, Report Danish Atomic Energy Commission Risø-M-1732 Roskilde, Denmark (1974).

[51]) T. B. Johansson, R. E. Van Grieken, J. W. Nelson and J. W. Winchester, Anal. Chem. **47** (1975) 855.

[52]) R. L. Walter, R. D. Willis, W. F. Gutknecht, J. M. Joyce, Anal. Chem. **46** (1974) 843.

[53]) T. A. Cahill, Proc. 3rd Conf. on *Application of small accelerators*, vol. 1 (1974) p. 184.

[54]) A. W. Herman, L. A. McNelles and J. L. Campbell, Int. J. Rad. Isotop. **24** (1973) 677.

[55]) R. D. Vis and H. Verheul, J. Radioanal. Chem. **27** (1975) 447.

[56]) F. C. Jundt, K. H. Purser, H. Kubo and E. A. Schenk, J. Histochem. Cytochem. **22** (1974) 1.

[57]) H. Kubo, Nucl. Instr. and Meth. **121** (1974) 541.

[58]) R. C. Bearse, D. A. Close, J. J. Malanify and C. J. Umbarger, Anal. Chem. **46** (1974) 499.

[59]) F. G. Resmini, A. D. Backer, D. J. Clark, E. A. McClatchie and R. De Siomiarski, Nucl. Instr. and Meth. **74** (1969) 261.

[60]) E. J. Feldt and C. J. Umbarger, Nucl. Instr. and Meth. **103** (1972) 341.

[61]) T. C. Chu, V. R. Navarrete, K. Kaji, G. Izawa, T. Shiokawa, K. Ishii, S. Morita and H. Tawara, J. Radioanal. Chem., in press.

[62]) L. Shabason, B. L. Cohen, G. H. Wedberg and K. C. Chau, J. Appl. Phys. **44** (1973) 4749.

[63]) M. Ahlberg, G. Johansson and K. Malmqvist, Nucl. Instr. and Meth., **131** (1976) 377.

[64]) J. M. Khan, D. L. Potter and R. D. Worby, Phys. Rev. **139** (1965) A1735.

[65]) L. Quaglia and G. Weber, Bull. Soc. Roy. Sci. Liège, **40** (1971) 54.

[66]) D. I. Bales, R. R. Landolt and W. E. Toll, Advan. X-ray Anal. **18** (1975) 299.

[67]) W. Beezhold, Thin Solid Films **19** (1973) 387.

[68]) J. Grönwall, Report LUNP 7308 (1973), Lund Institute of Technology, Lund, Sweden (In Swedish).

[69]) G. G. Seaman and K. C. Shane, Nucl. Instr. and Meth. **126** (1975) 473.

[70]) P. Horowitz and L. Grodzins, Science **189** (1975) 795.

[71]) T. B. Pierce, P. F. Peck and D. R. A. Cuff, Nucl. Instr. and Meth. **67** (1969) 1.

[72]) D. M. Poole and J. L. Shaw, 5th Int. Congress on *X-ray optics and microanalysis* (eds. G. Möllenstedt and K. H. Gaukler; Springer Verlag, Berlin, 1969) p. 319.

[73]) J. A. Cookson and F. D. Pilling, Report AERE-R 6300 (1970), Atomic Energy Research Establishment, Harwell, England.

[74]) M. Peisach, D. A. Newton, P. F. Peck and T. B. Pierce, J. Radioanal. Chem. **16** (1973) 445.

[75]) Z. H. Cho, M. Singh and A. Mohabbatizadeh, IEEE Trans. Nucl. Sci. **NS-21** (1974) 622.

[76]) F. Goulding and J. M. Jaklevic, Ann. Rev. Nucl. Sci. **23** (1973) 45.

[77]) H. A. Liebhafsky, H. G. Peiffer, E. H. Winslow and P. D. Zemany, *X-rays, electrons and analytical chemistry* (Wiley-Interscience, New York, 1972).

[78]) J. V. Gilfrich, Advan. X-ray Anal. **16** (1973) 1.

[79]) R. Dewolfs, R. De Neve and F. Adams, Anal. Chim. Acta **75** (1975) 47.

[80]) H. D. Fetzer and D. L. Parker, Metallography **7** (1974) 253.

[81]) H. Malissa, M. Grasserbauer and E. Hoke, Mikrochim. Acta Suppl. **5** (1974) 465.

[82]) K. Hardy, Florida Int. U., Miami, Florida, USA, private communication.

[83]) J. S. Hansen, J. C. McGeorge, D. Nix, W. D. Schmidt-Ott, I. Unns and R. W. Fink, Nucl. Instr. and Meth. **106** (1973) 365.

[84]) J. L. Campbell and L. A. McNelles, Nucl. Instr. and Meth. **98** (1972) 433.

[85]) R. Woldseth, *X-ray energy spectrometry* (Kevex Corporation, Burlingame, California, USA, 1973).

[86]) J. L. Campbell, B. H. Orr, A. W. Herman, L. A. McNelles, J. A. Thomson and W. Brian Cook, Anal. Chem. **47** (1975) 1542.

[87]) J. M. Jaklevic, F. S. Goulding and D. A. Landis, IEEE Trans. Nucl. Sci. **NS-19** no. 3 (1972) 392.

[88]) H. Thibeau, J. Stadel, W. Cline and T. A. Cahill, Nucl. Instr. and Meth. **111** (1973) 615.

[89]) J. T. Routti and S. G. Prussin, Nucl. Instr. and Meth. **72** (1969) 125.

[90]) V. Valković, R. B. Liebert, T. Zabel, H. T. Larson, D. Miljanić, R. M. Wheeler and G. C. Phillips, Nucl. Instr. and Meth. **114** (1975) 573.

[91]) J. P. Thomas, L. Porte, J. Engerrau, J. C. Viola and J. Tousset, Nucl. Instr. and Meth. **117** (1974) 579.

[92]) H. C. Kaufmann and R. Akselsson, Advan. X-ray Anal. **18** (1975) 353.

[93]) J. A. Bearden, Rev. Mod. Phys. **39** (1967) 78, reproduced in *Handbook of chemistry and physics* (ed. R. C. West; Chemical Rubber Co., Cleveland, Ohio 44128, USA).

[94]) A. W. Herman, L. A. McNelles and J. L. Campbell, Nucl. Instr. and Meth. **109** (1973) 429.

[95]) G. Johansson and K. Malmqvist, Report LUNP 7402 (1974), Lund Institute of Technology, Lund, Sweden (in Swedish).

[96]) K. K. Nielsen, M. W. Hill and N. F. Mangelson, Advan. X-ray Anal. **19** (1976) 511.

[97]) J. R. Rhodes and C. B. Hunter, X-ray Spectrom. **1** (1972) 113.

[98]) R. D. Giauque, L. Y. Goda and R. B. Garrett, Report LBL-2951, Lawrence Berkeley Laboratory (UC-11, TID-4500-R61).

[99]) T. G. Dzubay and R. O. Nelson, Advan. X-ray Anal. **18** (1975) 619.

[100]) R. E. Van Grieken and F. C. Adams, X-ray Spectrometry **5** (1976) 61; R. E. Van Grieken and F. C. Adams, Advan. X-ray Anal. **19** (1976) 339.

[101]) M. Ahlberg, R. Akselsson, D. Brune and J. Lorenzen, Nucl. Instr. and Meth. **123** (1975) 385.

[102]) K. Ishii, S. Morita, H. Tawara, T. C. Chu, H. Kaji and T. Shiokawa, Nucl. Instr. and Meth. **126** (1975) 75.

[103]) M. E. Alexander, E. K. Biegert, J. K. Jones, R. S. Thurston, V. Valković, R. M. Wheeler, C. A. Wingate and T. Zabel, Int. J. Rad. Isotop. **25** (1974) 229.

[104]) J. L. Campbell, A. W. Herman, L. A. McNelles, B. H. Orr and R. A. Willoughby, Advan. X-ray Anal. **17** (1974) 457.

[105]) G. H. Wedberg, K.-C. Chau, B. C. Cohen and J. O. Frohliger, Environ. Sci. Techn. **8** (1974) 1090.

[106]) D. C. Camp, A. L. Van Lehn, J. R. Rhodes and A. H. Pradzynski, X-ray Spectrom. **4** (1975) 123.

[107]) R. D. Lear, H. A. Van Rinsvelt and W. R. Adams, Advan. X-ray Anal. **19** (1976) 521.

[108]) D. C. Camp, J. A. Cooper and J. R. Rhodes, X-ray Spectrom. **3** (1974) 47.

[109]) R. E. Van Grieken, T. B. Johansson, J. W. Winchester and L. A. Odom, Z. Anal. Chem. **275** (1975) 343.

[110]) R. M. Wheeler, R. B. Liebert, T. Zabel, R. P. Chatuverdi, V. Valković, G. C. Phillips, P. S. Ong and E. L. Cheng Med. Phys. **1** (1974) 68.

[111]) T. A. Cahill, R. G. Flocchini, P. J. Feeney and D. J. Shadoan, Nucl. Instr. and Meth. **120** (1974) 193.

[112]) T. J. Gray, R. Lear, R. J. Dexter, F. N. Schwettmann and K. C. Wiemer, Thin Solid Films **19** (1973) 103.

[113]) J. F. Chemin, I. V. Mitchell and F. W. Saris, J. Appl. Phys. **45** (1974) 532 and J. Appl. Phys. **45** (1974) 537.

[114]) J. A. Cairns, A. D. Marwick and I. V. Mitchell, Thin Solid Films **19** (1973) 91.

[115]) S. K. Perry and F. P. Brady, Nucl. Instr. and Meth. **108** (1973) 389.

[116]) J. A. Cooper, Nucl. Instr. and Meth. **106** (1973) 525.

[117]) J. V. Gilfrich, P. G. Burkhalter and L. S. Birks, Anal. Chem. **45** (1973) 2002.

[118]) K. Willers, Report LUNP 7209 (1972), Lund Institute of Technology, Lund, Sweden (in Swedish).

[119]) T. B. Johansson, R. E. Van Grieken and J. W. Winchester, Proc. 2nd Int. Conf. on *Nuclear methods in environmental research*, Columbia, Missouri (1974) p. 356.

[120]) R. G. Flocchini, D. J. Shadoan, T. A. Cahill, R. A. Eldred, P. J. Feeney and G. Wolfe, Advan. X-ray Anal. **18** (1975) 579; R. G. Flocchini, T. A. Cahill, D. J. Shadoan, S. J. Lange, R. A. Eldred, P. J. Feeney, G. W. Wolfe, D. C. Simmeroth and J. K. Suder, Environm. Sci. Techn. **10** (1976) 76.

[121]) J. B. Barone, T. A. Cahill, R. G. Flocchini and D. J. Shadoan, submitted to Atm. Environm.

[122]) T. A. Cahill and P. J. Feeney, Report UCD-CNL 169, University of California, Davis; P. J. Feeney, T. A. Cahill, R. G. Flocchini, R. A. Eldred, D. J. Shadoan and T. Dunn, J. Air Poll. Control Assoc. **25** (1975) 1145.

[123]) J. Azevedo, R. G. Flocchini, T. A. Cahill and P. R. Stout, J. Environm. Quality **3** (1974) 171.

[124]) R. E. Van Grieken, T. B. Johansson, R. Akselsson, J. W. Winchester, J. W. Nelson and K. R. Chapman, Atm. Environm. **10** (1976) 571.

[125]) T. B. Johansson, R. E. Van Grieken and J. W. Winchester, J. Geophys. Res., **81** (1976) 1039.

[126]) J. W. Winchester, D. L. Meinert, J. W. Nelson, T. B. Johansson, R. E. Van Grieken, C. Orsini, H. C. Kaufmann and R. Akselsson, Proc. 2nd Int. Conf. on *Nuclear methods in environmental research*, Columbia Missouri (1974) p. 385.

[127]) K. A. Hardy, R. Akselsson, J. W. Nelson and J. W. Winchester, Environm. Sci. Techn. **10** (1976) 176.

[128]) R. Akselsson, C. Orsini, D. L. Meinert, T. B. Johansson, R. E. Van Grieken, H. C. Kaufmann, K. R. Chapman, J. W. Nelson and J. W. Winchester, Advan. X-ray Anal. **18** (1975) 588.

[129]) D. L. Meinert, M. S. Thesis (Florida State University, June 1974); D. L. Meinert and J. W. Winchester, submitted to J. Geophys. Res.

[130]) T. B. Johansson, R. E. Van Grieken and J. W. Winchester, J. Recherches Atmosphériques **8** (1974) 761.

[131]) B. Jensen and J. W. Nelson, Proc. 2nd Int. Conf. on *Nuclear methods in environmental research*, Columbia, Missouri (1974) p. 366; J. W. Nelson, B. Jensen, G. G. Desaedeleer, K. R. Akselsson and J. W. Winchester, Advan. X-ray Anal. **19**, (1976) 403.

[132]) K. R. Akselsson, K. A. Hardy, G. G. Desaedeleer, J. W. Winchester, W. W. Berg, T. B. Vander Wood, J. W. Nelson, Advan. X-ray Anal. **19** (1976) 415.

[133]) G. G. Desaedeleer, J. W. Winchester, R. Akselsson, K. A. Hardy and J. W. Nelson, Trans. Am. Nucl. Soc. **21** (Suppl. 3, 1975) 36.

[134]) R. Akselsson, G. Johansson, K. Malmqvist, J. Frismark and T. B. Johansson, Proc. 2nd Int. Conf. on *Nuclear methods in environmental research*, Columbia, Missouri (1974) p. 395. (See also ref. 95).

[135]) T. B. Johansson, R. Akselsson, M. Ahlberg, G. Johansson and K. Malmqvist, Trans. Am. Nucl. Soc. **21** (Suppl. 3, 1975) 31; K. Malmqvist, G. Johansson, R. Akselsson and T. B. Johansson, Report LUNP 7508, Lund Institute of Technology, Lund, Sweden, (in Swedish); T. B. Johansson, M. Ahlberg, R. Akselsson, G. Johansson and K. Malmqvist, J. Radioanal. Chem. **32** (1976) 207.

[136]) M. W. Hill, D. J. Eatough, L. D. Hansen, K. K. Nielsen, N. F. Mangelson and T. J. Smith, Trans. Am. Nucl. Soc. **21** (Suppl. 3, 1975) 35.

[137]) G. G. Desaedeleer and J. W. Winchester, Environm. Sci. Techn. **9** (1975) 971.

[138]) R. Akselsson, G. Desaedeleer, T. B. Johansson and J. W. Winchester, Ann. Occup. Hyg. (submitted).

[139]) H. A. Van Rinsvelt, F. E. Dunnam, J. P. Russell and W. E. Bolch, Proc. 3rd Conf. on *Application of small accelerators*, vol. 1 (1974) p. 148.

[140]) C. H. Lochmüller, J. Galbraith, R. Walter and J. Joyce, Anal. Lett. **5** (1972) 943; C. H. Lochmüller, J. W. Galbraith and R. L. Walter, Anal. Chem. **46** (1974) 440.
[141]) R. L. Walter, R. D. Willis and W. F. Gutknecht, Proc. 3rd Conf. on *Application of small accelerators*, vol. 1 (1974) p. 189.
[142]) N. F. Mangelson, M. W. Hill, K. K. Nielsen, D. J. Eatough, J. J. Christensen and R. M. Izatt, submitted to Anal. Chem.
[143]) C. J. Umbarger and J. J. Malanify, Int. J. Appl. Rad. Isotop. **23** (1972) 381.
[144]) H. A. Van Rinsvelt, R. Duerkes Jr., R. Levy and H. L. Cromroy, Florida Entomologist **56** (1973) 286; R. Levy, H. A. Van Rinsvelt and H. L. Cromroy, Florida Entomologist **57** (1974) 269.
[145]) P. Holst, Report LUNP 7407, Lund Institute of Technology, Lund, Sweden (in Swedish).
[146]) E. Fjerdingstad, K. Kemp, E. Fjerdingstad and L. Vanggaard Arch. Hydrobiol. **73** (1974) 70; E. Fjerdingstad, K. Kemp and E. Fjerdingstad, Arch. Hydrobiol. **74** (1974) 150.
[147]) S. A. Murray, T. A. Cahill, K. N. Paulson and A. R. Spun, Comm. Soil. Sci. Plant Anal. **6** (1975) 33.
[148]) J. M. Stanford, R. D. Willis, R. L. Walter, W. F. Gutknecht and J. Autonovics, Rad. Environm. Biophys. **12** (1975) 175.
[149]) R. K. Jolly, G. Randers Pehrson, S. K. Gupta, D. C. Buckle and H. Aceto Jr., Proc. 3rd Conf. on *Application of small accelerators*, vol. 1 (1974) p. 203.
[150]) V. Valković, D. Rendić and G. C. Phillips, Environm. Sci. Techn. **9** (1975) 1150.
[151]) N. F. Mangelson, G. M. Allison, D. J. Eatough, M. W. Hill, R. M. Izott, J. J. Christensen, J. R. Murdock, K. K. Nielsen and S. L. Welch, Proc. *Trace substances in environmental health VII* (1973) p. 369; N. F. Mangelson, K. K. Nielsen, M. W. Hill, D. J. Eatough and L. D. Hansen, Proc. 3rd Conf. on *Application of small accelerators*, vol. 1 (1974) p. 163.
[152]) J. W. Mandler and R. A. Semmler, Proc. 3rd Conf. on *Application of small accelerators*, vol. 1 (1974) p. 173.
[153]) K. Honda, S. Shishido, T. Suzuki, H. Kubo and R. Chiba, Tokoku J. Exp. Med. **117** (1975) 89.
[154]) M. Ahlberg and R. Akselsson, Int. J. Appl. Rad. Isotop. **27** (1976) 279.
[155]) G. Larsson, Dept. of Nucl. Physics, Lund Institute of Technology, Lund, Sweden, Report LUNP 7406 (1973) (in Swedish).
[156]) G. Demortier, J. Radioanal. Chem. **24** (1975) 47.
[157]) A. G. Strashinskii, G. K. Khomyakov, N. A. Skakun, N. V. Serykh and A. P. Klyucharev, Atomnaya Energiya **36** (1974) 401.
[158]) F. W. Reuter and H. P. Smith, J. Appl. Phys. **43** (1972) 4228.
[159]) L. C. Feldman, J. M. Poate, F. Ermanis and B. Schwartz, Thin Solid Films **19** (1973) 81.
[160]) W. Pabst, Nucl. Instr. and Meth. **120** (1974) 543 and **124** (1975) 143.
[161]) M. Ahlberg, Nucl. Instr. and Meth. **131** (1976) 381.
[162]) M. Ahlberg, R. Akselsson, B. Forkman and G. Rausing, Archaeometry **18** (1976) 39.
[163]) W. Pabst and K. Schmid, X-ray Spectrom. **4** (1975) 85.
[164]) M. Poncet and C. Engelmann, Analysis **3** (1975) 283.
[165]) R. A. Martin, G. G. Seaman and A. Ward, Cereal Chem. **52** (1975) 138.
[166]) P. Richard, M. Senglaub, B. Johnson and C. F. Moore, Appl. Phys. Lett. **21** (1972) 13.
[167]) P. G. Burkhalter, A. R. Knudson, D. J. Nagel and K. L. Dunning, Phys. Rev. **A6** (1972) 2093.
[168]) G. Deconninck, LARN Report 741.
[169]) R. G. Hurley and E. W. White, Anal. Chem. **46** (1974) 2234.
[170]) Y. Gohsi, O. Hirao and I. Suzuki, Advan. X-ray Anal. **18** (1975) 406.
[171]) E. A. Wolicki, NRL Report 7477 (1972) Naval Research Laboratory, Washington.
[172]) T. A. Cahill, R. Sommerville and R. Flocchini, Proc. of *Nuclear methods in environmental research* (1971) p. 26.
[173]) J. W. Nelson, I. Williams, T. B. Johansson, R. E. Van Grieken, K. R. Chapman and J. W. Winchester, IEEE Trans. Nucl. Sci. **NS-21**, no. 1 (1974) 618.
[174]) J. W. Nelson, J. W. Winchester and R. Akselsson, Proc. 3rd Conf. on *Application of small accelerators*, vol. 1 (1974) p. 139; J. W. Nelson and D. L. Meinert, Advan. X-ray Anal. **18** (1975) 598.
[175]) W. Beezhold, in Int. Symp. on *Silicon materials*, Sci. Technol. **2** (1973) 437.
[176]) G. A. Bissinger, A. B. Baskin, B.-H. Choi, S. M. Shafroth J. M. Howard and A. W. Waltner, Phys. Rev. **A6** (1972) 545.
[177]) T. J. Gray, R. Lear, R. J. Dexter, F. N. Schwettmann and K. C. Weimer, Thin Solid Films **19** (1973) 103.
[178]) K. Ishii, S. Morita, H. Tawara, H. Kaji and T. Shiokawa, Phys. Rev. **A10** (1974) 774.
[179]) H. Tawara, K. Ishii, S. Morita, H. Kaji, C. N. Hsu and T. Shiokawa, Phys. Rev. **A9** (1974) 1617.
[180]) N. A. Khelil and T. J. Gray, Phys. Rev. **A11** (1975) 893.
[181]) F. D. McDaniel, T. J. Gray and R. K. Gardner, Phys. Rev. **A11** (1975) 1607.
[182]) H. Tawara, K. Ishii, S. Morita, H. Kaji and T. Shiokawa, Phys. Rev. **A11** (1975) 1560.
[183]) R. P. Chaturverdi, R. M. Wheeler, R. B. Liebert, D. J. Miljanić, T. Zabel and G. C. Phillips, Phys. Rev. **A12** (1975) 52.
[184]) K. Ishii, S. Morita, H. Tawara, H. Kaji and T. Shiokawa, Phys. Rev. **A11** (1975) 119.
[185]) H. Tawara, Y. Hachiga. K. Ishii and S. Morita, Phys. Rev. **A13** (1976) 572.
[186]) M. Milazzo and G. Riccobono, Phys. Rev. **A13** (1976) 578.
[187]) J. R. Chen, J. D. Reber, D. J. Ellis and T. E. Miller, Phys. Rev. **A13** (1976) 941.
[188]) C. G. Soares, R. D. Lear, J. T. Sanders and H. A. Van Rinsevelt, Phys. Rev. **A13** (1976) 953.

The literature survey was terminated in January 1976.